ELECTRICAL–THERMAL MODELING FOR ELECTRICAL ASSEMBLIES USING THE FINITE ELEMENT METHOD

by

Samy Y. Hilali

Submitted in Partial Fulfillment of the Requirements

for the degree of

Master of Science in Engineering

in the

Mechanical Engineering

program

12/2/94

Advisor Date

12/1/94

Advisor Date

12/2/94

Dean of the Graduate School Date

YOUNGSTOWN STATE UNIVERSITY

December, 1994

ELECTRICAL–THERMAL MODELING FOR ELECTRICAL

ASSEMBLIES USING THE FINITE ELEMENT METHOD

by

Samy Y. Hilali

I hereby release this thesis to the public. I understand this thesis will be housed at the Circulation Desk of the University library and will be available for public access. I also authorize the University or other individuals to make copies of this thesis as needed for scholarly research.

Signature:

12/13/94

Student Date

Signature:

12/14/94

Advisor Date

Dec. 13, '94

Advisor Date

12/15/94

Committee Member Date

12/22/94

Committee Member Date

1/3/95

Dean of Graduate Graduate Studies Date

To my wife Azza

and

my daughter Sarra

ABSTRACT

The Finite Element Analyses (FEA) method is used to perform coupled Electrical – Thermal analyses of automotive electrical assemblies. An assembly consisting of a fuse, terminal and electrical wires is evaluated in the study. A procedure to conduct the analyses using the Patran 3 Finite Element Modeling software and the ABAQUS FEA software is developed and used to perform the analyses. The analyses is conducted on every component of the assembly individually and also on the complete assembly. The analyses includes a representative finite element model for the electrical as well as the thermal contact resistance between the terminal and the fuse blades.

The analyses procedure consists of three steps. The first step is to perform the electrical analyses in order to obtain the electric current density and voltage potential. The second step is to calculate the power distribution based on the current density. The third step is the heat transfer analyses using the power distribution as input to obtain the temperature distribution in the electrical assembly.

Experimental study for the components of the assembly as well as the assembly itself is completed. Hand calculations are performed for the electrical wire in order to validate the procedure. The results of the experimental work and the FEA analyses are tabulated and compared. The FEA results correlates well with the experimental study for the components and the assembly. The FEA results also correlate well with the hand calculations in the case of the electrical wire analyses.

ACKNOWLEDGEMENTS

With humbleness and gratitude, I thank God for providing me the strength to complete this endeavor. The guidance of Dr. Bor-Jenq Wang, my advisor from Packard Electric Division of General Motors Corporation, was instrumental in making this work possible. My thanks, respect and appreciation go to him. I thank Dr. Hyun W. Kim, my advisor from Youngstown State University, for helping me bring this thesis to completion. The time he spent in reviewing the manuscript and providing comments is greatly appreciated. I also thank Dr. Frank Tarantine and Dr. Ganesh Kudav for serving on my committee, reviewing the manuscript and providing feedback. Also, I thank my colleague, Mr. Robert Rimko from Packard Electric for his help and feedback with the finite element analysis. I thank my colleagues Mr. Robert Vennetti and Mr. Steve Vu for helping me conduct the experiments. I also would like to thank Mr. Wayne Martorana, my supervisor at Electronic Data Systems, for taking the time to review the manuscript and provide valuable editorial comments.

I am grateful to Electronic Data Systems Corporation and Packard Electric Division of General Motors Corporation for providing computer hardware, software licenses and lab facilities and equipment that enabled this work to come to fruition.

Finally, I thank my wife Azza and my daughter Sarra to whom I dedicate this thesis, for their patience, love and encouragement, especially during the difficult times.

TABLE OF CONTENTS

LIST OF SYMBOLS

SYMBOL	DEFINITION	UNITS OF REFERENCE
a	Contact spot radius	mm
A	Wire cross sectional area, apparent contact area	mm^2
A_c	Solid to solid contact area	mm^2
A_v	Void area	mm^2
d	Wire insulation outer diameter	mm
h,h_c	Convection heat transfer coefficient, contact coefficient	$W/mm^2\,^\circ C$
h_r	The radiation heat transfer coefficient,	$W/mm^2\,^\circ C$
I	Current	A
J	Current density	A/mm^2
k	Coefficient of thermal conductivity	$W/mm\,^\circ C$
L,l	Length	mm
L_g	Thickness of the void space	mm
P	Power	W
q	Heat transfer rate	W
R,R_e	Electric resistance	Ω
R_c	Convection resistance	$^\circ C/W$
R_r	Radiation resistance	$^\circ C/W$

SYMBOL	DEFINITION	UNITS OF REFERENCE
ΣR_{th}	Total thermal resistance	°C/W
R_{th}	Thermal resistance	°C/W
T_i	The temperature on the wire core surface	°C
T_o	The wire insulation surface temperature	°C
T_∞	Room temperature	°C,°K
T_s	Surface temperature	°K
V,v	Voltage	V
ε	Emissivity	–
ρ	Electrical resistivity	Ω mm
σ	Electrical conductivity	1/Ω mm
σ	Stephan-Bolzman constant	–

LIST OF FIGURES

LIST OF TABLES

INTRODUCTION

Automotive Electrical Systems have grown more complex than ever. One trend has been towards Electrical Assemblies carrying more power devices and using smaller spaces. The increased power concentration leads to higher temperatures in the assemblies. Reliability of the Electrical Assemblies lessens when local/system temperature increases significantly. Particularly, when several applications are placed in such a hostile environment as an engine compartment, the Electrical Assemblies are subject to catastrophic failures.

A typical Electrical Assembly consists of connections (wires, terminals,etc.), devices (fuses, relays, etc.), plastic layers and housing. Before thermal analyses can be conducted, the heat generation (primarily the Joule heat) in the connections and devices due to electrical current needs to be determined. Given the applied current, the Joule heat can be readily calculated if the conductor geometry is uniform. However, for a non-uniform geometry, electrical analyses is required to determine the current /voltage potential thus, the power (Joule heat) distribution. In addition to the power distribution determination, the thermal analyses model needs to be constructed with proper conduction, convection and radiation boundary conditions.

Thermal analyses can be conducted through either the analytical approach or the numerical method. While the analytical approach is limited to some generic geometries, the finite difference[1], finite element[2], and boundary element[3,4] methods of the numerical technique can provide solutions for problems with complex geometry. Due to the complex geometric nature of Electrical Assemblies, the Finite Element Method will be used. Patran3 and Abaqus software at Packard Electric is utilized. The proper boundary conditions for Electrical Assemblies is also investigated in this thesis work.

---

[1]J.A. Andrews, L.M. Mahalingam, and H.M. Berg, "Thermal Characteristics of 16–pin and 40–pin Plastic DIP's," IEEE Trans. Components, Hybrids, and Manufacturing Technology, CHMT–4, Dec. 1981, pp.455–461

[2]D.L. Waller, L.R. Fox and R.J. Hannemann, "analyses of Surface Mount Thermal and Thermal Stress Performance," IEEE Trans. Components, Hybrids, and Manufacturing Technology, CHMT–6, Sept. 1983, pp.257–266

[3]C.C. Lee, A.L. Palisoc, and J.M.W. Baynham, "Thermal Analysis of Solid State Devices using Boundary Element Method," IEEE Trans. Electron Devices, 35, pp.1151–1153

[4]C.C. Lee and A.L. Palisoc, "Thermal Analysis of Semiconductor Devices," Topics in Boundary Element Research, Ed. by C.A. Brebbia, Berlin, Germany: Springer–Berlag, Vol. 7, 1990, pp.12–33

CHAPTER I

ANALYSES APPROACH

Introduction

Automotive electrical centers often contain sub-assemblies that consist of a fuse, terminal and wire. The temperature distribution of the sub-assembly as a result of applying a certain amount of current is of interest. In the following chapters, this sub-assembly will be examined in detail to determine its temperature rise. The analyses approach of this thesis is to model each component of the assembly separately then assemble them together for a combined evaluation. The Finite Element Method (FEM) is used for analyses.

The current passed through an electrical assembly produces heat. In an automobile, if the heat generated is excessive, it can cause device failures and sometimes fires. Thermal management considerations in the design of such products is important not only for reliability, but also for safety. A traditional way of designing such assemblies is based on a factor of safety and experience. After the preliminary design, a prototype part is manufactured. This prototype is then tested and its temperature rise determined. If the temperature rise falls within the design guidelines then the design process is said to be complete. But in reality, many iterations are required to come up with the final reliable and safe product. The problem is that this design approach takes too long and is too costly. For a world as competitive as today's this is simply, unacceptable.

The designer requires a tool that can predict design faults quickly and with reliability. If such tool exists, it can reduce the number of design iterations and prototype cost. Most of the analyses performed today on such products starts by assuming a uniform heat generation distribution in the conductive parts of the assembly and goes on to predict the surface temperature. The inaccuracies in such analyses is due to the uniform heat distribution load assumption used in the thermal analyses. The distribution of the heat generated in a conductor is dependent on the geometry and thus the electrical current distribution. In this thesis work the analyses starts at an earlier step. It accurately determines the electric current distribution first and then computes the power distribution for any given geometry. The analyses method is an iterating one that couples both electrical and thermal finite element analyses using P3/PATRAN™ [5] and ABAQUS® [6] software programs.

Approach

When a current is passed through a wire or a conductor it produces heat. An explanation to this phenomena lies in the understanding of electric current. In an electric field the electric charge is carried in metallic conductors by electrons. The movement of these free electrons form the electric current. The electric field loses power in order to move the free electrons. This power is converted into heat and is given by Joule's law[7]:

$$P = I^2 R \tag{1}$$

[5] P3/PATRAN is a trademark of PDA Engineering.

[6] ABAQUS is a rigestered trademark of Hibitt, Karlsson, and Sorensen, Inc..

[7] John D. Kraus, Electromagnetics, (New York: McGraw-Hill, Inc., Fourth Edition, 1992), p. 185.

Where P is the Joule heating power,

I is the electrical current, and,

R is the resistance in Ω

Determining such power requires the determination of the current density for irregular geometry. The analyses approach used in this thesis applies the finite element method in determining the current density, voltage potential and temperature distribution of electrical assemblies. The finite element models presented are constructed using the Patran 3 software. The heat transfer analyses capabilities in the ABAQUS Finite Element analyses (FEA) software is used to perform both the electrical and thermal analyses. The analogy between the thermal and electrical quantities are shown in Table 1. The output of the electric analyses is the voltage potential and current density. Once the current density for the various elements in the model is determined, the power distribution is calculated using equation (1). This power is used in a subsequent finite element heat transfer analyses and applied as a thermal load. The result of the FEA is a temperature distribution of the assembly being analyzed. The FEA results were obtained starting with the electrical analyses using the electrical resistivity at an arbitrary temperature. The maximum surface temperature obtained from the thermal analyses step was used to calculate the new electrical resistivity and the analyses was reiterated. When the difference between the final temperature and the temperature used for the electrical resistivity was less than 1%, the solution was called to have converged.

In Chapter II, the analyses of an insulated wire is performed. The simple geometry of the wire makes it a good candidate for proof of concept of the method used in the analyses approach. An automotive fuse model is constructed and analyzed in chapter III while an electrical terminal model is built and analyzed in chapter IV. In chapter V, the complete assembly is considered for analyses including the interface resistance between the terminal and the automotive fuse. All finite element results are compared with experimental results. The experiments explained throughout the thesis were performed at the Packard Electric Division of General Motors' test facility in Warren Ohio.

TABLE 1

ELECTRICAL – THERMAL ANALOGY

Electrical quantity	Thermal quantity
Voltage, V	Temperature, T
Electrical conductivity, σ	Thermal conductivity, k
Current density, J	Heat flux,$-(k \cdot \nabla T)$

CHAPTER II

INSULATED WIRE ANALYSES

Introduction

Wires are very important components in an electrical assembly. They are the carriers of the power and signal to many electrical devices in the automobile. Understanding the thermal response of electrical wires in an automotive application is a key to the integrity of the entire system as well as the safety of the automobile occupants. The temperature distribution of the wire as a result of applying a certain current is of interest. This chapter outlines the electrical and thermal modeling of a 10-gauge electrical wire.

The Finite Element Analyses Method is used to model the electrical wire. A three dimensional Finite Element Model is constructed. Electrical analyses is first performed to obtain voltage potential, current density and power distribution. Thermal analyses is then carried out to determine the temperature distribution of the wire surface. Hand calculation is completed to obtain the power and temperature distribution of the wire. An experiment to evaluate the thermal response of the wire is performed.

The approach taken is to model a long horizontal wire with its insulation material. Hand calculations, experimental data and FEA results are compared and found to be in good agreement. The analyses is conducted with the finite element method using

P3/PATRAN finite element modeling and ABAQUS FEA software programs on Hewlett Packard model 735 engineering workstation.

Hand Calculations

The objective of the hand calculations is to determine the wire surface temperature in order to compare with both the experimental and FEA results. One-dimensional analyses can be considered for an infinite length specimen with no temperature change expected in the axial direction. First, the power generated due to the electric current passing through the wire is calculated. After calculating the power, conduction, convection and radiation thermal resistances are calculated. Finally, the surface temperature is determined.

Wire Geometry

In order to proceed with the hand calculations, the wire geometry is first examined. The electrical wire considered has a length of a 910 mm with a cross sectional area of 5 mm^2. Such geometry can be considered to have an infinite length with no temperature change expected in the axial direction.

A cross section of the wire which shows the wire core, insulation and its geometric characteristics is shown in Figure 1 From the Figure, A_c is the copper core cross sectional area and is given to be 5 mm^2, r_o is the wire insulation core radius found to be 1.90 mm and r_i the copper core radius found to be 1.26 mm.

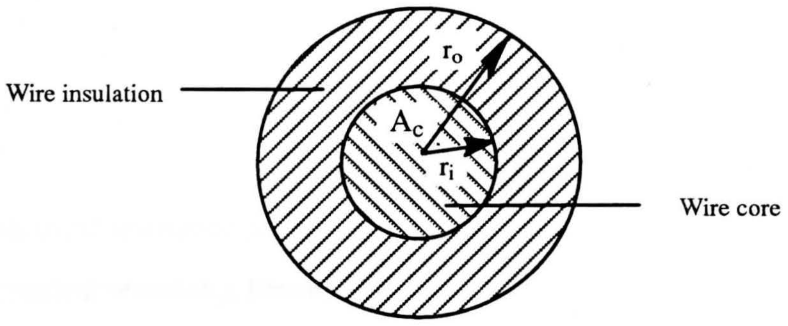

Fig. 1. Wire cross section

Electrical Analyses Calculations

When analyzing the wire's electrical characteristics we find that two parameters are of interest, the electrical resistance and the power generation. The objective of performing the electrical analyses calculations is to determine the above two parameters in the given geometry. This power distribution equals the Joule heating which acts as a heat source in the model. The Joule heating is later applied to the thermal analyses model as boundary conditions. When we examine the wire geometry we find that it has a constant cross sectional area. This means that the power distribution in the wire is constant because of the regular geometry shape. The following equation yields the value of the Joule heating power:

$$P = I^2 R \tag{2}$$

where P is the Joule heating power,

I is the electrical current, A and

R is the resistance, Ω

In order to determine the electrical resistance R, we employ the following equation[8]:

$$R = \frac{\rho \times l}{A} \tag{3}$$

Where R is the electrical resistance, Ω,

ρ is the electrical resistivity, Ωmm,

l is the wire length, mm and

A is the wire core cross sectional area, mm^2

The above two equations determine the power generated by the current passing through the electric wire. The mathematical calculations are given in Appendix A , equations number (23) and (24). Table 15 outlines the results of the calculations.

Thermal Analyses

For one dimensional heat transfer, equation[9] (42) serves as the governing equation. We calculate the equivalent thermal resistance then substitute in the equation in order to determine T_i:

$$q = P = \frac{T_i - T_\infty}{\Sigma R_{th}} \tag{4}$$

where q is the heat transfer rate, W

P is the Joule heating power, W

T_i is the temperature on the wire core surface, °C

---

[8] John D. Kraus, Electromagnetics, p. 187.

[9] Frank P. Incropera and David P. DeWitt, Fundamentals of Heat Transfer (New York: Wiley, 1981), p. 69.

T_∞ is the ambient temperature, °C and

ΣR_{th} is the total thermal resistance in the radial direction, °C/W

TABLE 2

ELECTRICAL ANALYSES HAND CALCULATION RESULTS

Parameter	Value
Electrical Resistance	0.04332Ω
Power	38.9880W

Heat is transferred through the wire by three means, conduction through the insulation material, free convection and radiation to the surrounding air. The total thermal resistance consist of the conduction, convection and radiation resistances. Both the convection and radiation resistances act in parallel while their equivalent resistance act in series with the conduction resistance. Figure 41 illustrates the thermal resistance of the wire.

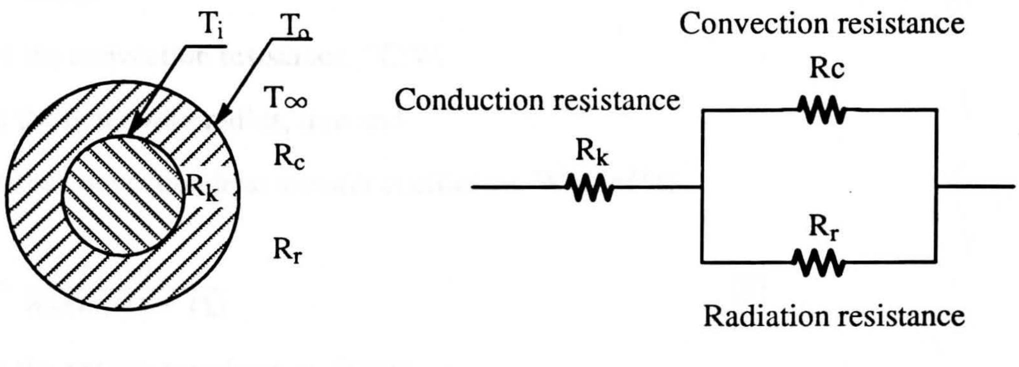

Fig. 2. Thermal resistance representation of the wire model

The total thermal resistance of the wire can be found from the following equation:

$$\Sigma R_{th} = R_K + \frac{R_c R_r}{R_c + R_r} \tag{5}$$

where R_k is the conduction resistance, °C/W,

R_c is the convection resistance, °C/W and

R_r is the radiation resistance, °C/W

Using equations (44), (45) and (46), the conduction[10], convection[11] and radiation[12] resistances can be calculated. The values of the resistances can then be substituted in equation (43) to compute the total thermal resistance.

$$R_k = \frac{\ln\left(\frac{r_o}{r_i}\right)}{2\pi L k} \tag{6}$$

where R_k is conduction resistance, °C/W

L is the wire length, mm

r_o is the outer wire radius, mm

r_i is the wire core or the inner insulation radius, mm and

k is the insulation material coefficient of thermal conductivity, W/mm°C

$$R_c = \frac{1}{2\pi L r_o h} \tag{7}$$

where R_c is the convection resistance, °C/W,

r_o is the outer wire radius, mm and

h is the convection heat transfer coefficient, W/mm²°C

$$R_r = \frac{T_o - T_\infty}{\sigma\varepsilon 2\pi L r_o (T_o^4 - T_\infty^4)} \tag{8}$$

where R_r is the radiation resistance, °C/W,

T_o is the wire outer surface temperature, °K,

[10]Incropera, Fundamentals, p.81.

[11]Incropera, Fundamentals, p.80.

[12]Incropera, Fundamentals, p.10.

T_∞ is the ambient temperature, °K,

σ is the Stephan-Bolzman constant,

ε is the material emissivity, and

r_o is the outer wire radius, mm

TABLE 3

VALUES OF WIRE THERMAL RESISTANCES

Resistance Type	Value °C/W
Conduction Resistance R_k	0.0399
Convection Resistance R_c	0.4600
Radiation Resistance R_r	1.8220
Total Resistance ΣR_{th}	0.4070

Next, the total thermal resistance is substituted in equation (42) to obtain T_i. After determining the value of T_i, conduction across the insulation material is evaluated and the insulation surface temperature T_o is determined using equation (47). The results of the wire temperature calculations are supplied in Table 17 while the calculations are provided in Appendix A.

$$q = \frac{2\pi Lk(T_i - T_o)}{\ln\left(\frac{r_o}{r_i}\right)} \tag{9}$$

where q is the heat transfer rate, W

T_i is the temperature on the wire core surface, °C and

T_o is the wire outer insulation surface temperature, °C

TABLE 4

TEMPERATURE DISTRIBUTION

Temperature Location	Value °C
Wire core surface, T_i	39.8
Insulation surface, T_o	37.3

Wire Experiment

Description

The objective of the experiment is to obtain the surface temperature of the wire to verify both hand calculations and FEA results. Surface temperature measurements of a horizontal electrical wire isolated from air movements around it were obtained. The wire ends were kept at a constant temperature while supplied by a steady current. Temperature measurements of the wire ends are later applied to the FEA model as boundary conditions.

A specimen 910 mm long of 10-gauge wire was prepared. To isolate the wire from the surrounding air movements, it was placed inside a tube. The tube dimensions were 900 mm long and 65 mm in diameter. Two heat sinks were connected to the wire ends in order to keep them at a constant temperature. An ambient thermometer was placed in the lab to measure the room temperature. An Inframatrics model 600 infrared imaging camera was used for surface temperature measurements.

Preparation

A window 13 mm wide was cut along the tube length and was covered with clear thin plastic wrap for visualization and temperature measurement. The tube was fixed on a wooden board for portability. The wire was placed in the center of the tube with its ends outside. The wire ends were soldered to the heat sinks. Two end wires were soldered on the two heat sinks for power supply purposes. The infrared camera was aimed at the wire in order to gather the sample data required. The photo picture in Figure 42 shows the wire experiment set up.

Experiment Procedure and Results

Three different variations of the experiment were conducted using electrical current values of 30, 45, and 55 A. After the set up was completed, the power supply was turned on. The temperature of the wire stabilized after about twenty minutes signaling that it has reached steady state. The heat sink temperature was monitored to confirm constant temperature. The infrared camera was directed at the wire and focused. Thirteen different data points on the wire were pre-marked and samples gathered. The temperature of the two soldered wire ends and the two heat sinks were also recorded. A set of three readings were taken for every data point. The average of the three readings was calculated and reported in Table 7. While conducting the 30 A experiment, the electrical resistance was measured and found to be 4.01 mΩ. The device used to measure the electrical resistance was the HP model 4328A ohmmeter.

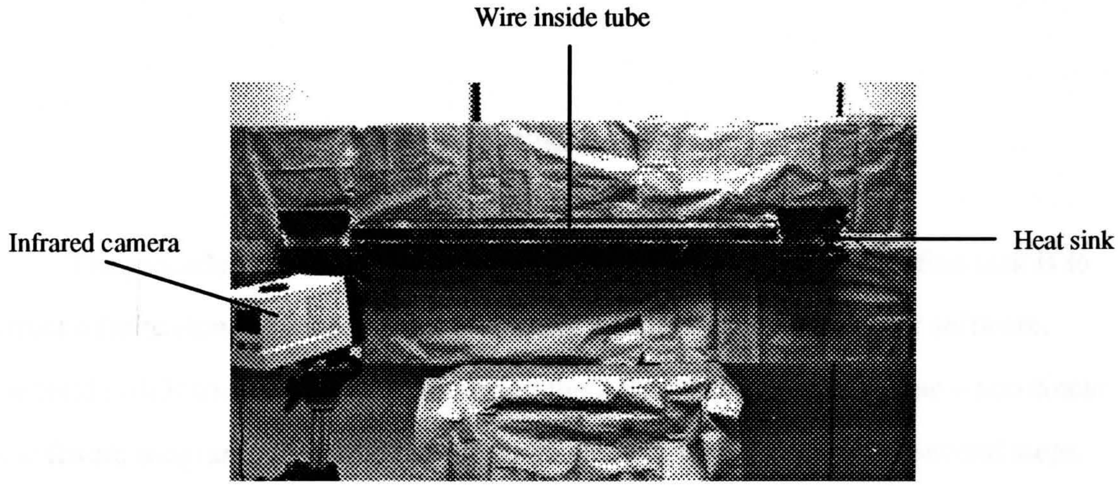

Fig. 3 The wire experiment set up.

The Finite Element Analyses

The procedure of conducting the FEA consists of two tasks. The first task is to construct a finite element model using the Patran 3 finite element modeling software. The second task is to analyze the model using the ABAQUS general purpose – non-linear FEA software program. Constructing the finite element model consists of several steps. A geometry model that represents the part being modeled is first prepared. A layer of a finite number of smaller elements is created on top of the geometry model. The elements that make up the layer are called the finite element mesh. Next, material properties of the part are assigned to the Finite Element Mesh. While forces and boundary conditions can be applied to either the mesh or the geometry, it is preferred to be applied to the geometry. This saves modeling time later when a more refined mesh layer is required. An input file that describes the model is then prepared by the modeling software and may be edited by the user for specific parameters. This input file is then submitted to the analyses software to be solved.

The coupled electrical–thermal analyses is an iterative process that consist of three steps. The first step is to determine the current density and the voltage potential. This is done by performing an electrical FEA. Very few software programs on the commercial market offer electrical current loading. Also, the programs that offer such capabilities are very expensive. Hence, the method introduced in this thesis can serve as an alternative tool for solution of the coupled electrical–thermal FEA problems. Here, the analogy between electrical and thermal systems is utilized and the thermal FEA software is used. The temperature-dependent electrical resistivity is calculated initially based on an arbitrary temperature chosen by guessing the surface temperature. The second step is to calculate the power distribution for every element in the FEA model based on the electrical current distribution obtained from the first step and the electrical resistivity. In the third step the temperature distribution is calculated using the thermal FEA software based on the power distribution calculated in step two. The maximum temperature in the model is compared to the initial temperature for convergence. The convergence criteria used in this thesis is 1%. If convergence is not achieved, the electrical resistivity is recalculated based on the new temperature distribution and the analyses is repeated.

The Wire Geometry Model

The geometry is constructed using Patran 3 software. The type of element to choose when creating the finite element model later has to be considered at this stage. The wire core is represented by five solid geometric entities while the insulation is represented by four solid geometric entities. Figure 4 shows a cross section in the geometry model. The wire core has a square entity in the middle to prevent wedge elements from forming during the meshing step. Each solid geometric entity has a length of 910 mm. A wire core cross sectional area of 5 mm^2 is modeled. The overall wire diameter with insulation is 3.8 mm.

The Wire Finite Element Mesh Model

The geometry is meshed using three-dimensional, 20-noded hexahedral elements. Uniform mesh is created throughout the wire length. Although 8-noded hex elements are sufficient for many applications, the 20-noded element is chosen because it follows the cylindrical nature of the wire surface better than the 8-noded element. The copper core is modeled using 12 hexahedral elements per cross section while the plastic insulation is modeled using 8 hexahedral elements per cross section. The total number of elements and nodes in the model is 180 and 915 respectively.

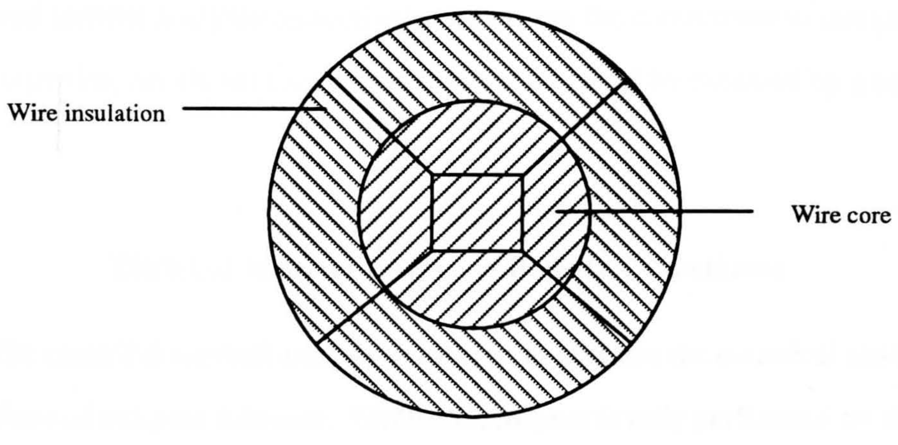

Fig. 4 The finite element geometry model

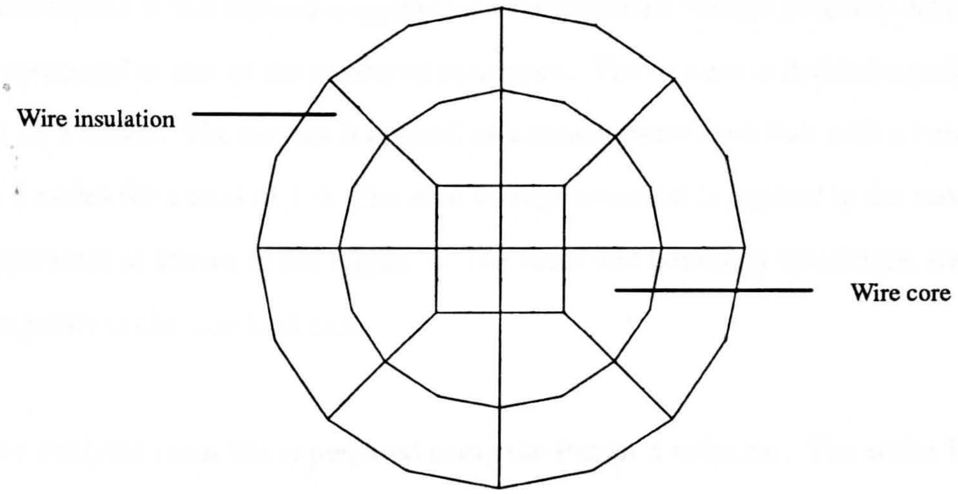

Fig. 5 Two dimensional view of the finite element wire mesh

Figure 5 illustrates a cross section of the finite element mesh model for both the wire core and the insulation. After creating the mesh, it is necessary to clean the duplicate nodes that lie on top of each other on the adjacent geometric solids boundaries. Eliminating the duplicate nodes process is called equivalencing in the Patran 3 software.

The absence of duplicate nodes prevent solver errors later during the analyses phase. Next, the elements are given the material properties of both the wire core and plastic insulation. The material properties are the electrical and the thermal conductivity for the electrical and thermal analyses respectively. To ensure the correctness of assigning material properties, an element attributes verification could be executed on a random element.

Electrical Analyses Loads and Boundary Conditions

The electrical-thermal analogy is utilized to perform the electrical analyses using the thermal analyses software. Electrical analyses is only performed on the conductive part of the model, the wire core. From Ohm's law, if the current applied equals 1 A, then the voltage drop equals the electric resistance. In order to verify the finite element model, a unit current is applied and the resultant voltage potential across the wire is compared to that of the measured resistance. The current is divided equally and applied on 8 nodes. The current is applied as a concentrated heat flux with a value of 0.125 A on 8 nodes for a total of 1 A. The zero voltage potential is applied to the model as zero temperature as shown in the Figure. 6 The loads and boundary conditions are combined together under one load case.

The analyses input file is prepared using the Patran 3 software. The entire FEA model is considered with the combined load case mentioned above. Several output options can be specified. The solution method chosen is a linear static, steady state solution. The results of interest are the heat flux at the element centroid and the nodal temperatures which represent the current density and the voltage potential respectively.

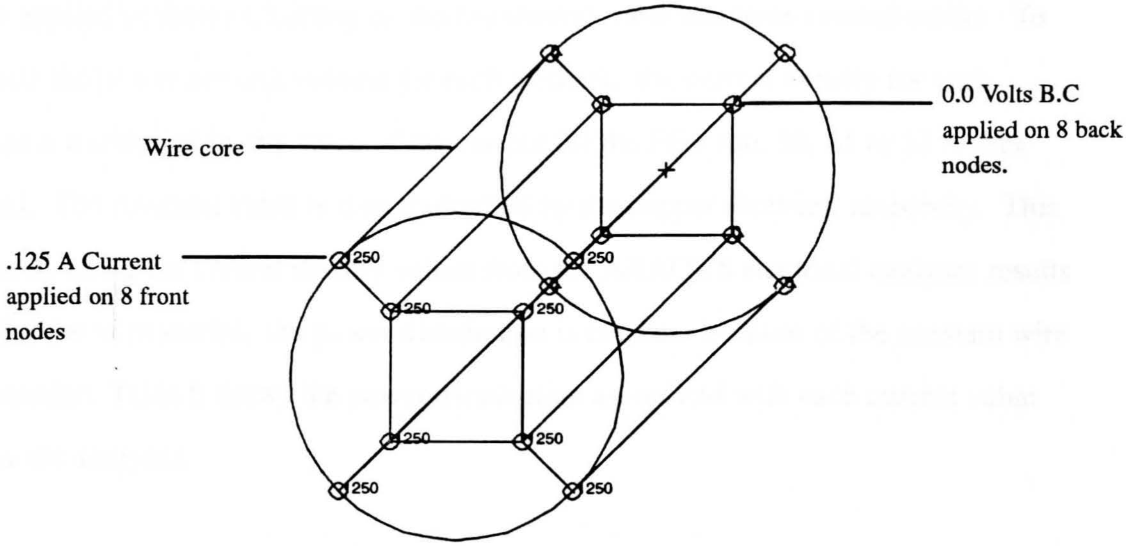

Fig. 6 Electrical analyses loads and boundary conditions

Electrical Analyses Results

The voltage drop for the 30 A FEA run is found to be 0.0335 v as illustrated in Table 5. This translates to a 16.46% difference from the measurement of 4.01 mv obtained by the HP model 4328A ohmmeter during the 30A experiment. The current distribution is also obtained and is found to be a constant value of 0.2006 A/mm^2. For a quick check, we multiply this value by the wire cross sectional area. This results in 1 A which is the sum of the applied current at the nodes.

Power Distribution Calculation

When electric current flows through a resistance, the power developed is proportional to the square of the current and directly proportional to the resistance.[13] The second step in the electrical thermal analyses procedure is to calculate the power generated in the model due to the current passing through. The power per unit volume

[13]Theodore Baumeister, Eugene A. Avallone and Theodore Baumeister III, Mark's Standard Handbook for Mechanical Engineers (New York: McGraw–Hill, Inc. 1978), p. 15–10.

can be applied as thermal loading on the hexahedral mesh elements created earlier. To calculate the power per unit volume for each element, the current density for each element is multiplied by the value of the current for the FEA run, 30, 45 or 55 A then squared. The resultant value is then multiplied by the copper electrical resistivity. This is done by using the current density values from the ABAQUS electrical analyses results file. For the wire model, the power distribution is constant because of the constant wire cross section. Table 6 shows the power distribution associated with each current value used in the analyses.

TABLE 5

FEA ELECTRICAL ANALYSES WIRE RESULTS

Parameter	Value
Voltage potential at 30A	0.0335 v
Voltage potential 45A	0.0350 v
Voltage potential at 55A	0.0362 v
Current Density for 30, 45 and 55 amps	0.2006 A/mm^2

TABLE 6

WIRE POWER DISTRIBUTION RESULTS

Current, ampere	Power distribution, Watts per mm^3
30	0.666380E–3
45	0.156454E–2
55	0.241020E–2

Thermal Analyses Loads and Boundary Conditions

The third and final step in the procedure is the heat transfer analyses. In this step, the original finite element model used during the electrical analyses step is utilized. However, the loads, boundary conditions and material properties are modified. While in the electrical analyses step only the electrically conductive part in the model was used, in the heat transfer step the entire model including insulation is used. The boundary conditions on the opposite ends of the wire core are defined as constant temperatures. The constant temperatures are obtained from experimental results and are given in Table 7 as sold. 1 and sold. 2 temperatures. Convection and radiation boundary conditions are applied to the wire insulation surface. The temperature dependent convective heat transfer coefficient is defined according to the following equation[14]:

$$h_c = 1.32\left(\frac{\Delta T}{d}\right)^{1/4} \tag{10}$$

where h_c is the convective heat transfer coefficient, W/mm^2°C and

d is the wire insulation outer diameter, mm

The radiation boundary conditions are defined on the outer surface of the insulation by specifying the radiation heat transfer coefficient using the following equation[15]:

$$h_r = \frac{\sigma\varepsilon(T_s^4 - T_\infty^4)}{(T_s - T_\infty)} \tag{11}$$

where h_r is the radiation heat transfer coefficient, W/mm^2°C,

σ is the Stephan-Bolzman constant,

ε is the material emissivity,

[14]J.P. Holman, Heat Transfer (New York: McGraw-Hill, 1976), p. 253

[15]Incropera, Fundamentals, p.25

T_s is the surface temperature, °K, and

T_∞ is the ambient temperature, °K

The power generation per unit volume obtained during the power generation calculation step is applied to each element of the wire core part of the model. Finally, the thermal conductivity of both the copper core and that of the insulation is assigned to the geometry model. The temperature dependency of the thermal conductivity is taken into consideration. After making all the necessary changes for the model, the ABAQUS heat transfer input file is generated using the Patran 3 software and then submitted to ABAQUS for analyses.

Thermal Analyses Results

The ABAQUS results file is brought into the Patran 3 for post-processing. The temperature distribution of the wire insulation is shown in Table 7. The highest temperature measured was 36.56, 48.65, 57.95 °C for 30, 45 and 55 A currents respectively. There is a consistent agreement between this temperature and the temperature measured with the Infrared camera during the experiment. The temperature of the hottest region during the test had average measurements of 36.8, 52.6, and 65.9 °C for currents of 30, 45 and 55 amps respectively. The finite element analyses temperature results had a maximum difference of 12.23% of the experiment results. The maximum temperature obtained from the hand calculations was 37.3 °C at 30 A current. The FEA model has a difference of 1.98% with reference to hand calculations.

Discussion

The FEA results were obtained starting with the electrical analyses using the copper resistivity at an arbitrary temperature. The surface temperature obtained from the thermal analyses step was used to calculate the new electrical resistivity and the analyses was reiterated. When the difference between the final temperature and the temperature used for the electrical resistivity was less than 1%, the solution was said to have converged. In most cases convergence required only two steps. Narrowing the convergence criteria can produce better results, but not significantly better. The electrical analyses results shown in Table 5 show good correlation with the measured results of 4.01 m.Ω . Examining the thermal analyses results in Table 7 shows that the higher the temperature, the lower the accuracy of the solution. The results obtained from the FEA analyses show good correlation with experimental results and hand calculations. The convection coefficient of heat transfer used is in a general form for a cylinder, using the localized convection heat transfer coefficient would produce better results.

TABLE 7

WIRE TEMPERATURE DISTRIBUTION CORRELATION

current, Amps.	Method	Temperature, °C													
		Solder 1	T1	T3	T4	T6	TM	T7	T9	T10	T12	Solder 2	Sink 1	Sink 2	ambient
30	Test	24.7	32.3	35.1	36.3	36.5	36.8	36.4	36.1	35.3	32.4	24.7	23	23	24.5
	FEA	24.7	33.07	35.6	36.34	36.54	36.56	36.54	36.34	35.6	33.07	24.7			24.5
	diff. %	0	2.38	1.42	0.11	0.11	0.65	0.11	0.11	0.85	2.07	0			
45	Test	27.6	44.7	49.8	51.7	52.4	52.5	52.6	52.3	50.8	45.9	26.6	24	24	24.2
	FEA	27.6	42.96	47.22	48.35	48.62	48.65	48.62	48.33	47.15	42.7	26.6			24.2
	diff. %	0	3.89	5.18	6.48	7.21	7.33	7.57	7.59	5.81	6.1	0			
55	Test	28.8	54.3	61.9	64.9	65.5	65.8	65.9	65.6	63.4	56.0	28.1	25	24	23.1
	FEA	28.8	50.46	56.18	57.59	57.92	57.95	57.92	57.58	56.14	50.30	28.1			23.1
	diff %	0	7.07	9.24	11.26	11.57	11.93	12.11	12.23	11.45	10.18	0			

$T_{solder1}$ T1 T2 T3 T4 TM T5 T6 T7 T8 $T_{solder\ 2}$

CHAPTER III

AUTOMOTIVE FUSE ANALYSES

Introduction

Fuses are the primary circuit protection devices in automobiles. They are usually located inside the automobile fuse block or electrical center. The temperature rise of a fuse is an important design characteristic for the fuse block or the electrical center. This temperature rise must be determined during the design phase in order to assure that their integrity and reliability are not compromised. Fuse temperature rises because of the electrical current passing through. Sometimes, the thermal effects reach the maximum limit when the fuse current rating is reached. The fuse rated current has a value slightly lower than the fusing current.[16] After a period of time at the rated current, the fuse element melts causing the circuit to disconnect, thus, protecting other valuable elements such as motors and devices.

This chapter outlines the modeling and analyses of a 30 A automotive fuse without plastic housing. The finite element method is used to model the fuse. A two-dimensional finite element model is constructed. Electrical analyses is first performed to obtain voltage potential, current density and power distribution. Thermal analyses is then carried out to determine the temperature distribution. An experiment is performed to measure the temperature distribution of the fuse. The results of both the experimental work and the FEA are compared. The analyses is conducted utilizing the

[16] Fuses for Automotive applications (The Netherlands: Littelfuse Tracor B.V., Utrecht), p. 8.

P3/PATRAN finite element modeling and ABAQUS FEA software programs on Hewelett Packard model 735 engineering workstation.

Electrical Resistance Measurements

TABLE 8

AUTOMOBILE FUSE RESISTANCE MEASUREMENTS

Sample #	Value	Fuse Sample
1	0.0019 Ω	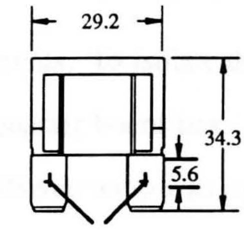
2	0.0019 Ω	
3	0.00192Ω	
4	0.00192Ω	
5	0.00185Ω	points of contacts
Average	0.00189Ω	

The electric resistance across the fuse blades is measured using a calibrated Hewlett Packard ohmmeter model number 4328A. Several samples were considered and readings were taken at room temperature. The measurements and their averages are shown in Table 8. The resistance is measured from the points of contacts between the fuse blade and the terminal and the average is found to be 1.89 mΩ. The location of the points of contacts is depicted in Table 8.

Fuse Experiment

Description

The objective of the experiment is to obtain the surface temperature of the fuse to verify the FEA results. Surface temperature measurements of a vertical fuse isolated from air movements around it were obtained. The fuse ends were kept at a constant temperature while supplied with a steady current. Temperature measurements of the fuse blades were later applied to the FEA model as boundary conditions.

The 30 A fuse was tested at 10, 20 and 30 A currents. To isolate the fuse from the surrounding air movements, it was placed in a small boaster board box. A window was cut in one side of the box for temperature readings. Plastic wrap was used to cover the window.

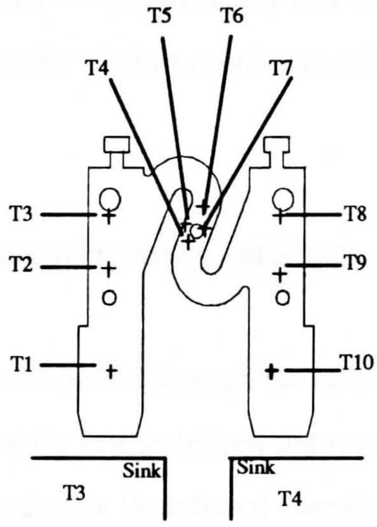

Fig. 7 Fuse temperature measurement locations

Two heat sinks were connected to the fuse in order to keep the two blades' ends at a constant temperature. The current was kept steady by manually adjusting the power supply while measuring the current across a shunt resistor throughout the experiment. An ambient thermometer was placed in the lab to measure the room temperature. For fuse temperature measurement, the inframatrics model 600 infrared imaging camera was used.

Preparation

The experiment components were assembled on a wooden board for portability. The board and the experiment set up is shown in Figure 8. First, the heat sinks were fixed to the board at such a distance so that the fuse would fit vertically with its two blades each fixed to a heat sink. The fuse ends were soldered to the heat sinks so that the fuse will stand vertically. Two end wires were soldered on the two heat sinks for power supply purposes. The boaster board box was placed on top of the fuse. The test assembly was placed on a counter and the power supply was connected. The infrared camera was turned on and aimed at the window opening in order to gather the sample data required.

Experiment Procedure and Result

Three different currents were passed through the fuse, 10, 20 and 30 A. After about 5 minutes, the temperature of the fuse stabilized and reached a steady state. The heat sink temperature was monitored using the infrared camera to confirm constant temperature. The infrared camera was directed at the fuse and focused. The different data points on the fuse were measured and sample readings gathered. The temperature of the two soldered fuse blades ends and the two heat sinks were also recorded. A set of three readings were taken for every data point. The average of the three readings was calculated and reported in Table 9.

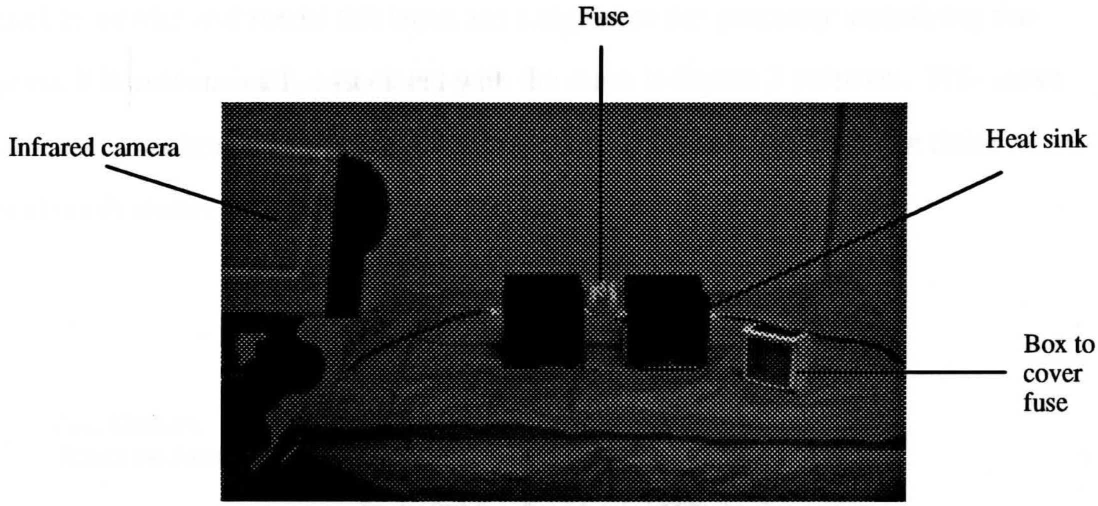

Fig. 8 The Fuse Experiment Set Up

The Finite Element Geometry Model

The metal conductor part of the fuse consists of three different regions. The first region consists of the two fuse blades where the fuse connects to the electrical terminal. The second area is a thickness transition area between the blades and the fuse element. The third area is the fuse element area. The geometry is constructed using Patran 3. A three-dimensional model is constructed. First, surfaces that make up the geometry is created and then thickness is assigned to complete the three dimensional model. Areas around the circles are constructed carefully for later mesh refinement. Figure 9 illustrates the geometric entities representing the fuse. The fuse material is assumed to be Zinc. The geometric entities are assigned electrical and thermal material properties for the electrical and thermal analyses respectively.

The Finite Element Mesh Model

The geometry is meshed as two dimensional shell elements. Finer mesh is created for areas of complex geometry than for areas of simple geometry. Because the material properties and model thickness are assigned to the geometry underlying the elements, it is automatically associated with the mesh in Patran 3 software. This saves valuable analyses time when the need to further refine the mesh arises. The finite element mesh model is shown in Figure 10.

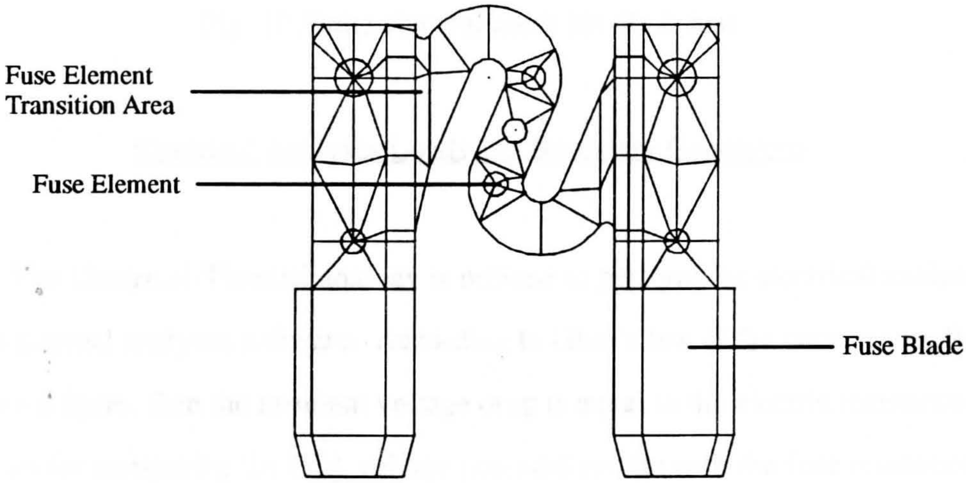

Fig. 9 Fuse geometry model

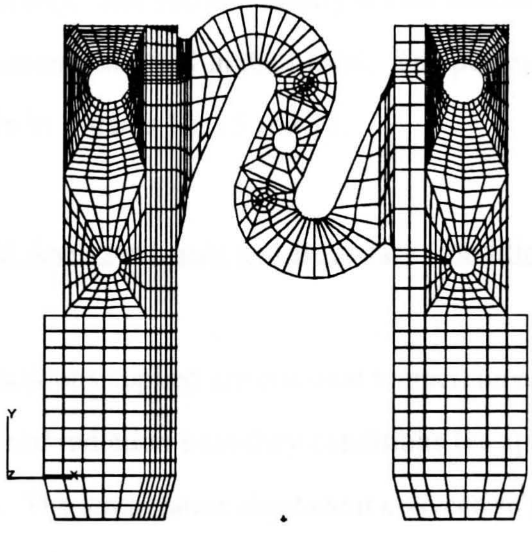

Fig. 10 Finite element mesh for 30 A fuse

Electrical Analyses Loads and Boundary Conditions

The Electrical-Thermal analogy is utilized to perform the electrical analyses using the thermal analyses software. According to Ohm's law, if the current supplied equals one ampere, then the resultant voltage drop is equal to the electric resistance. This allows for comparing the FEA voltage potential results with the fuse resistance measurements shown in Table 8. The boundary conditions applied to the model is a 1A current and a grounded point representing zero voltage. The current is applied on two nodes with a value of 0.5A as concentrated heat flux. The grounded points are specified as zero temperatures.

Electrical Analyses Results

The FEA voltage potential difference is found to be 2.0 mΩ at room temperature. This translates to a 5.82% difference from the measurement obtained by the Hewlett Packard ohm meter. Voltage potential is illustrated on figures 11, 14, and 17 for 10, 20 and 30 A respectively. The current density is also obtained and used to calculate the power distribution generated in the model. The power distribution for the different currents are shown in Figures 12, 15 and 18.

Thermal Analyses Loads and Boundary Conditions

The boundary conditions applied are constant temperature, convection and radiation. The convection and radiation boundary conditions are applied to the front and back faces of the elements. The temperature dependent convective heat transfer[17] coefficient taken to be:

$$h_c = 1.42\left(\frac{\Delta T}{L}\right)^{1/4} \tag{12}$$

where h_c is the convective heat transfer coefficient, W/mm^2°C and

L is the vertical dimension, mm

The radiation boundary conditions are defined on the outer surface of the insulation by specifying the radiation heat transfer coefficient using the following equation[18]:

$$h_r = \frac{\sigma\varepsilon(T_s^4 - T_\infty^4)}{(T_s - T_\infty)} \tag{13}$$

where h_r is the convective heat transfer coefficient, W/mm^2°C and

σ is the Stephan-Bolzman constant,

ε is the material emissivity,

---

[17]Holman, <u>Heat Transfer</u>, p. 253

[18]Incropera, <u>Fundamentals</u>, p.25

T_s is the surface temperature, °K,

T_∞ is the ambient temperature, °K

A constant temperature is applied to both the left and right blade edges. This temperature is obtained from the experimental procedure results. Table 9 shows the value of the temperature applied as sold. 1 and sold. 2 for the left and right blade edges respectively. The thermal load applied to the model is that of the joule power generated in the model due to the current density. The heat generation in watts per unit volume is applied to each element of the model.

Thermal Analyses Results

The temperature distribution of the fuse is depicted on Figures 13, 16 and 19 for 10, 20 and 30 A respectively. The FEA results are tabulated in Table 9 for the various current values. Table 9 also shows a comparison between the experimental and FEA results for approximately the same locations and currents. The accuracy of the FEA is calculated and depicted in the same Table. The accuracy of the finite element analyses is in good agreement with the the experimental results at low current rating. At high temperature the FEA results have values much higher than the experimental results.

Discussion

The difference in the FEA and experimental results can be attributed to several reasons. One of the reasons is that the location of infrared measurement is not exactly the same location as the FEA node. The measurement location falls only in the proximity of the node. Another reason is that the fuse is modeled with shell elements. Although the shell element takes a thickness property and the analyses is carried out as a solid model, the convection and radiation cannot be specified in ABAQUS off the side of the fuse 2–D shell elements. A model with 3-D solid elements would produce better results.

TABLE 9

RESULTS COMPARISON OF 30 A FUSE

Current	Meth-od	Temperature °C / Node number														
		T1/ 2380	T2/ 1751	T3/ 1543	T4/ 2540	T5/ 2557	T6/ 2570	T7/ 2583	T8/ 719	T9/ 916	T10/ 1447	sold.1	Sold2	Sink1	Sink2	Am-bient
10 Amps	Test	24.3	25.3	25.5	27.9	27.0	27.6	27.0	25.1	25.1	24.3	25.2	25.1	25.4	25.1	23.4
	FEA	25.59	26.23	26.62	30.13	30.19	30.02	30.23	26.15	26.14	25.53					
	% diff	5.31	3.68	4.39	7.99	11.81	8.77	11.96	4.18	4.14	5.06					
20 Amps	Test	28.0	31.7	33.3	44.4	39.9	41.5	39.7	30.8	31.5	28.5	26.8	27.5	26.0	25.5	24.6
	FEA	28.78	31.59	33.22	47.54	47.88	47.2	47.99	31.91	31.84	29.35					
	% diff	2.79	0.35	0.24	7.07	20.0	13.73	20.88	3.60	1.08	2.98					
30 Amps	Test	35.0	44.3	48.0	77.1	65.8	70.0	66.9	42.6	44.0	36.3	29.4	30.2	25.9	25.5	23.1
	FEA	33.93	40.27	43.96	77.44	78.28	76.64	78.56	40.60	40.49	34.67					
	% diff	3.06	9.10	8.42	0.44	18.97	9.49	17.43	4.69	7.98	4.49					

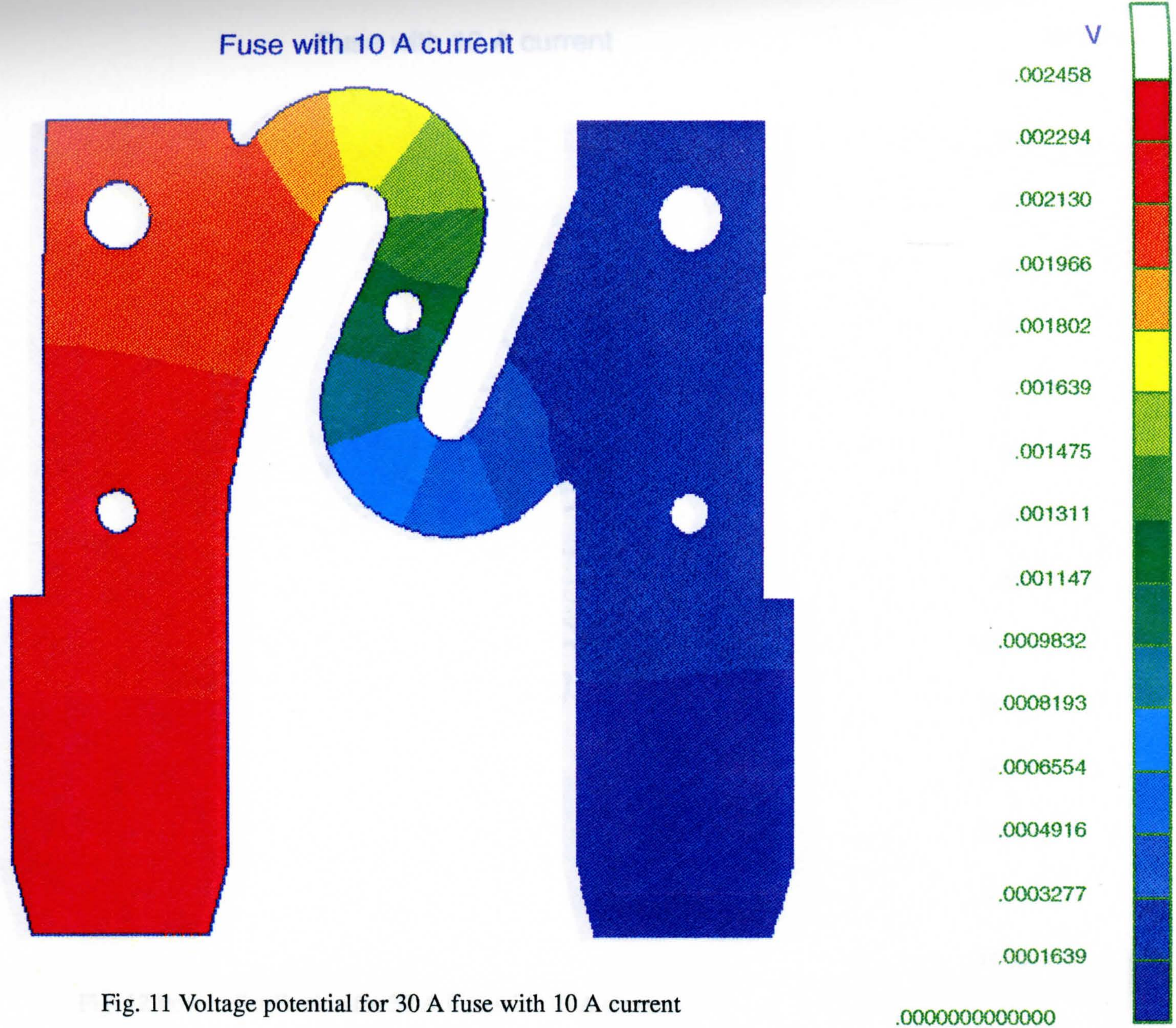

Fig. 11 Voltage potential for 30 A fuse with 10 A current

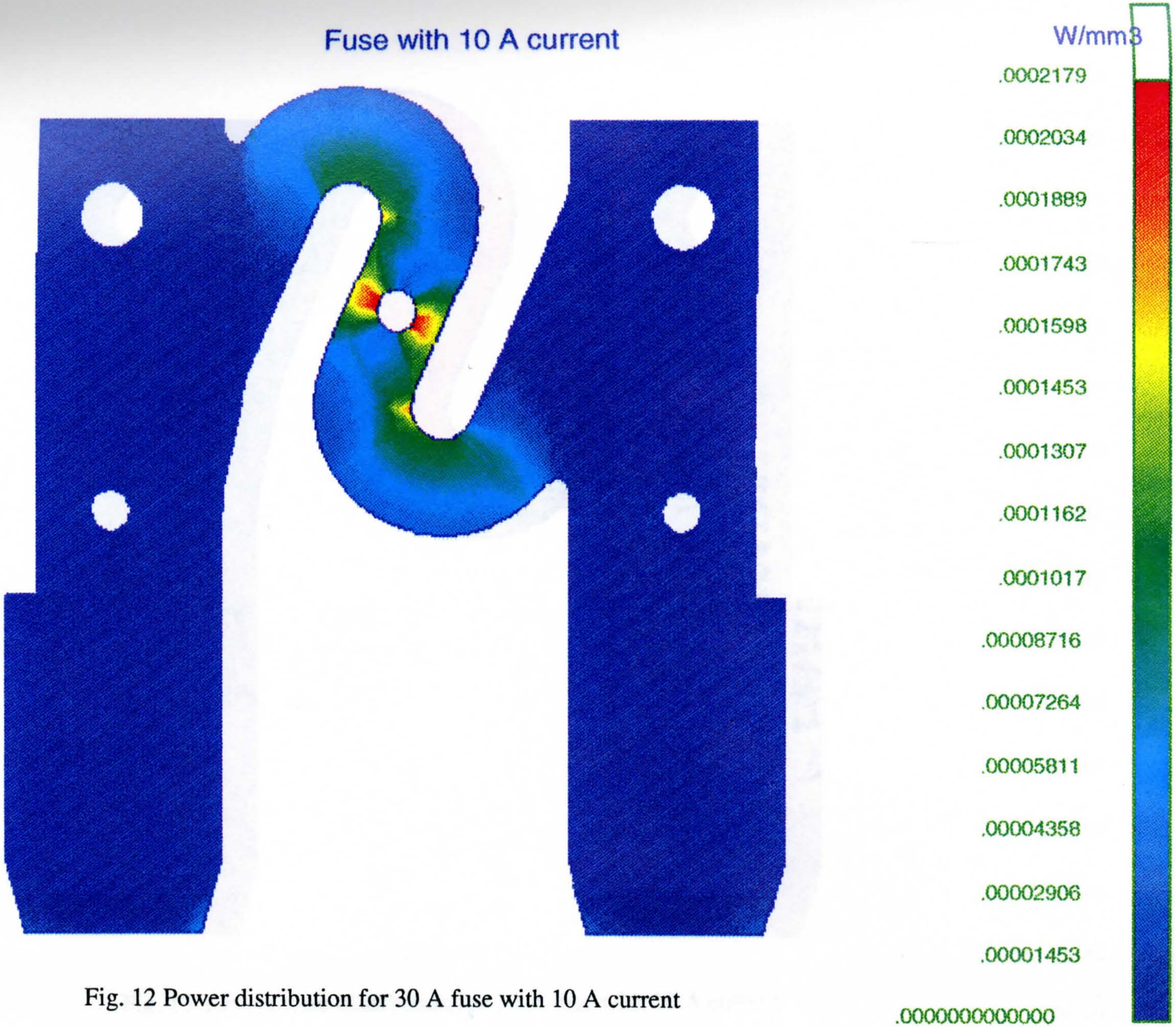

Fig. 12 Power distribution for 30 A fuse with 10 A current

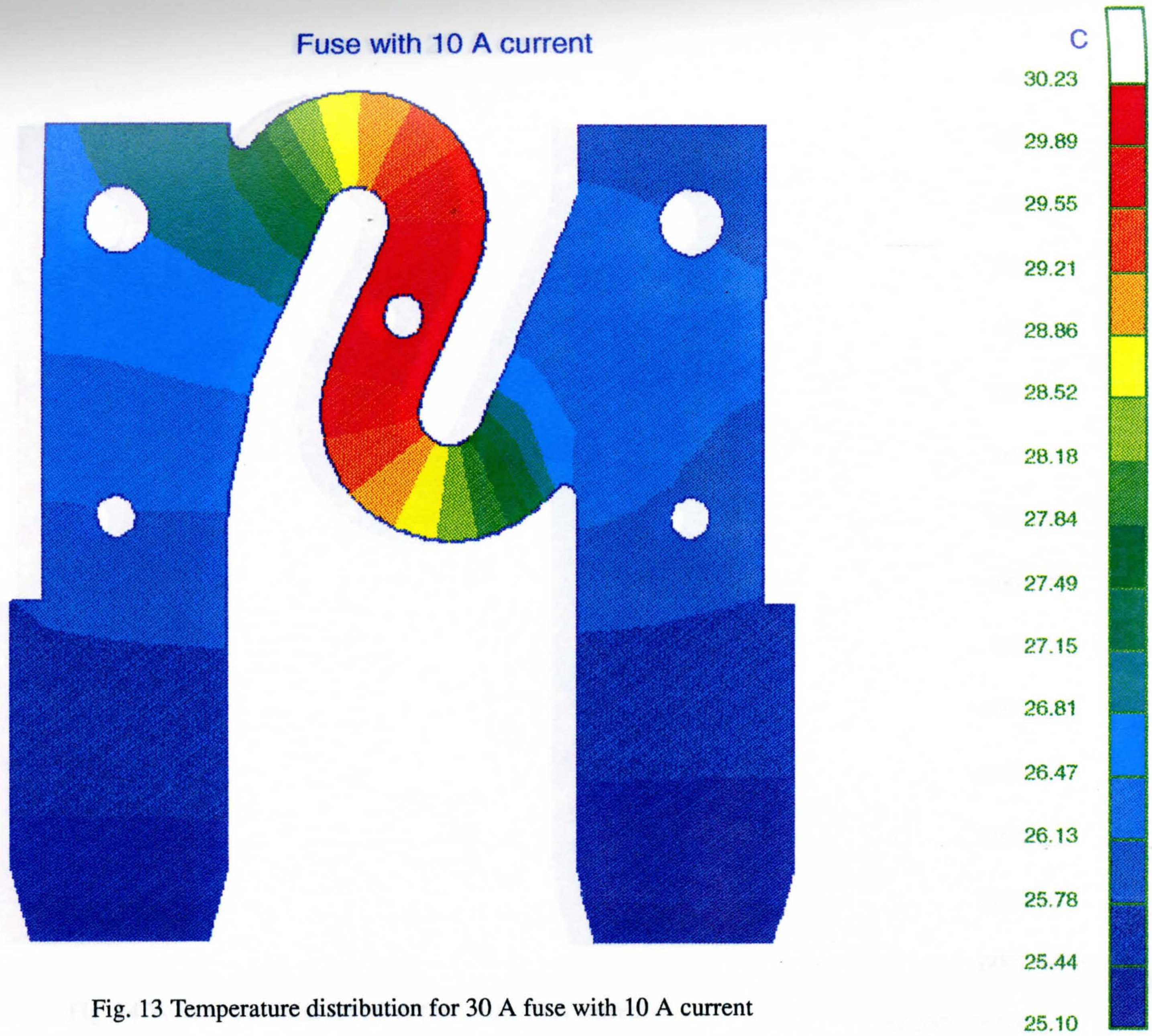

Fig. 13 Temperature distribution for 30 A fuse with 10 A current

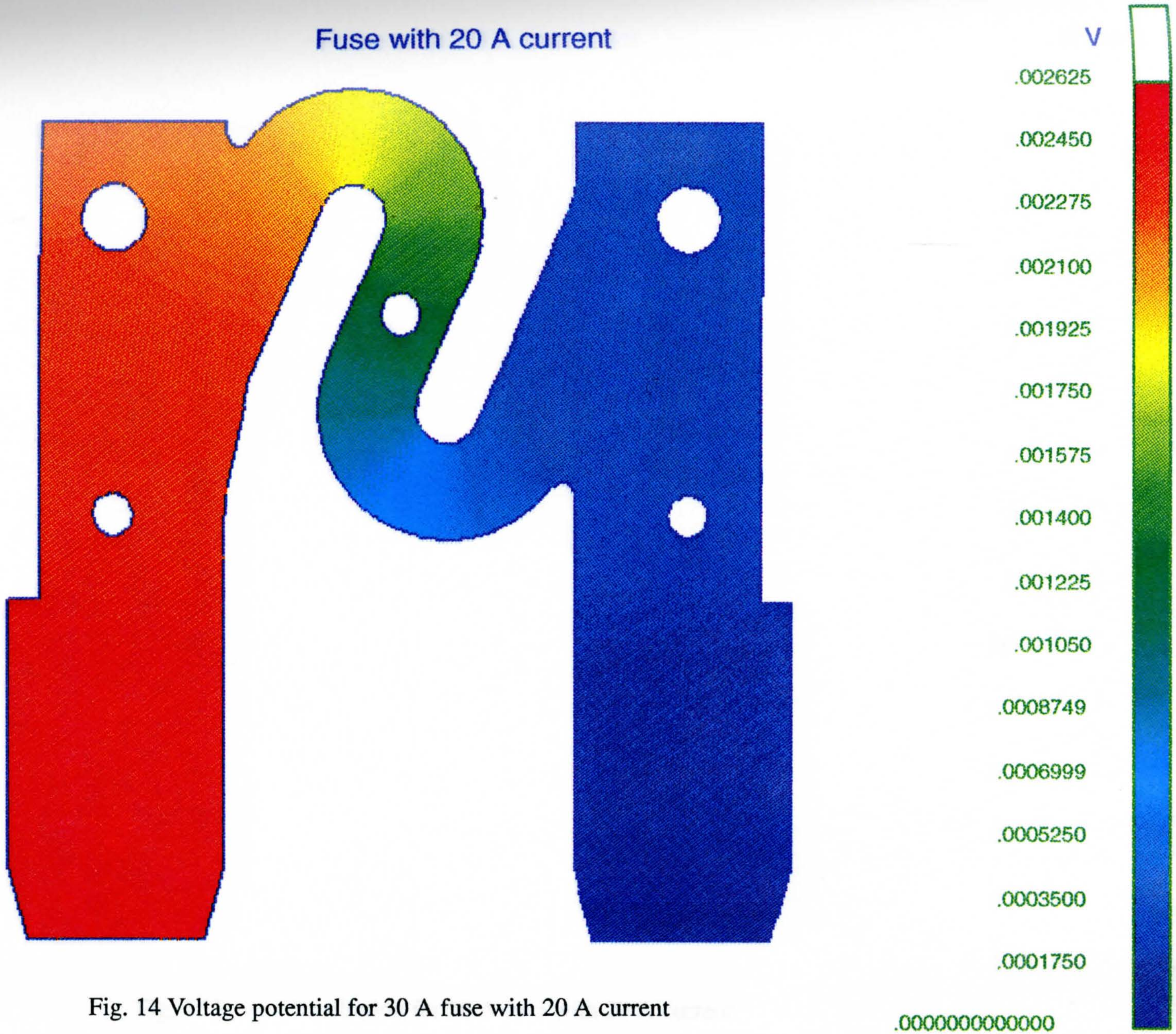

Fig. 14 Voltage potential for 30 A fuse with 20 A current

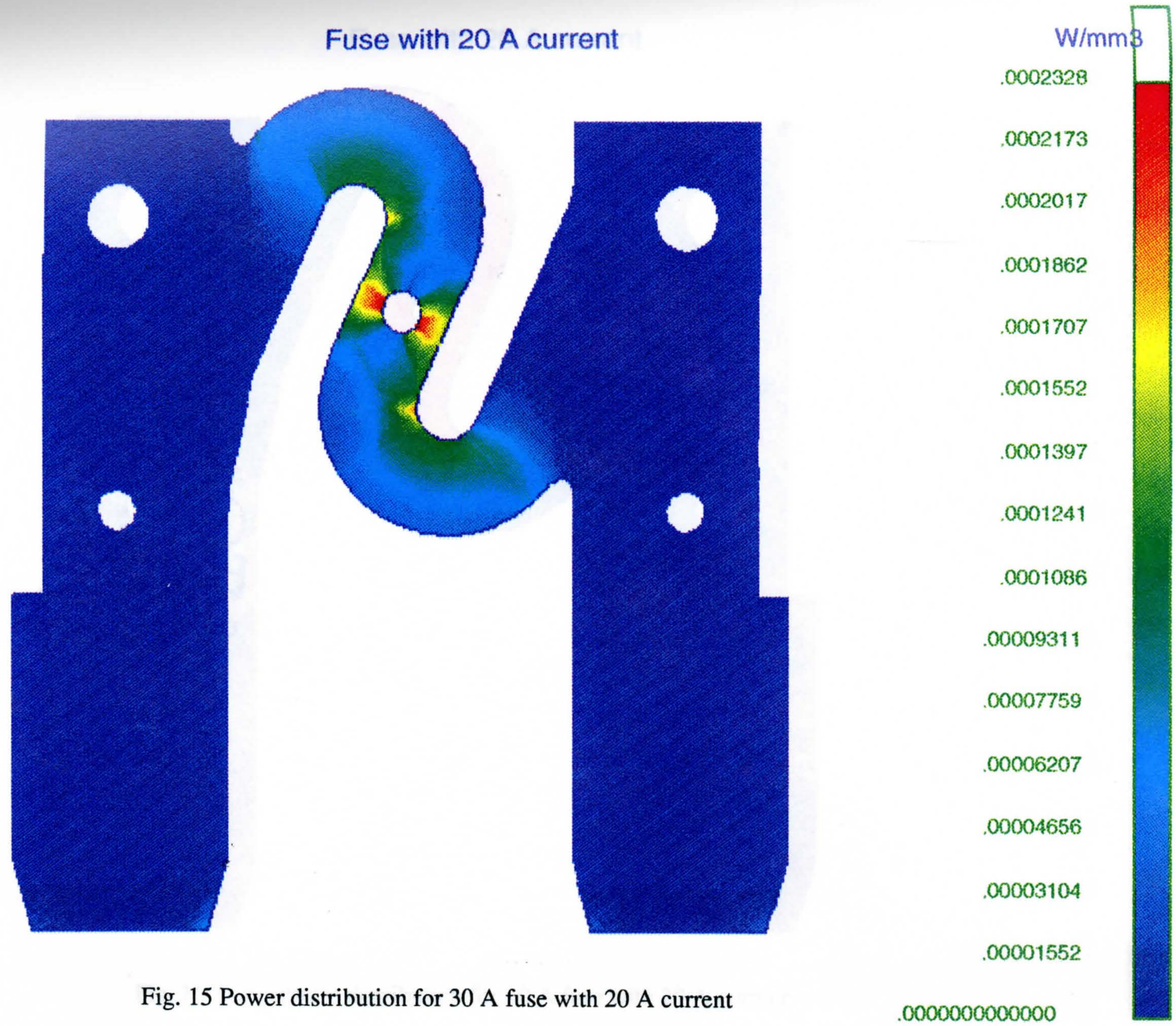

Fig. 15 Power distribution for 30 A fuse with 20 A current

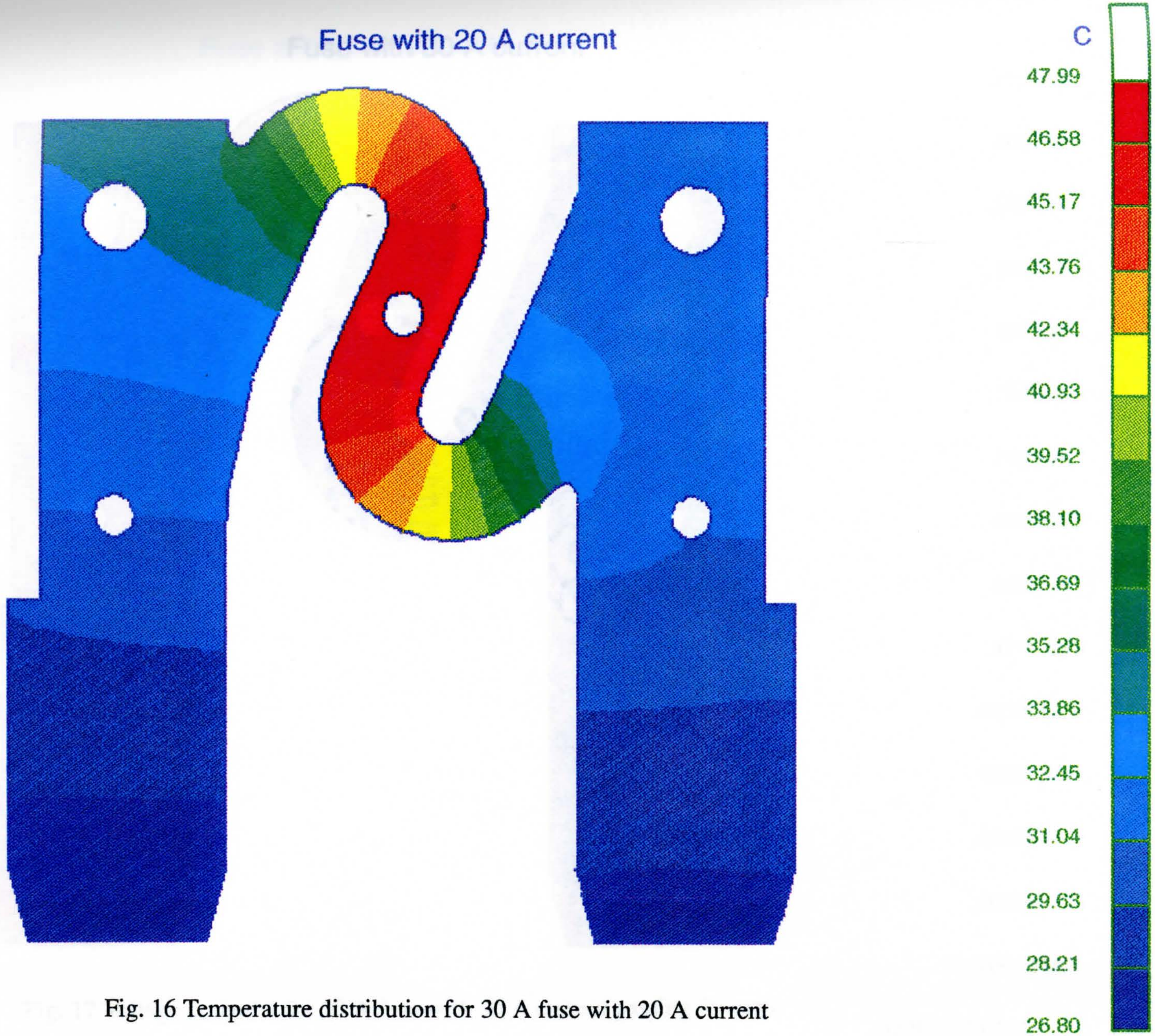

Fig. 16 Temperature distribution for 30 A fuse with 20 A current

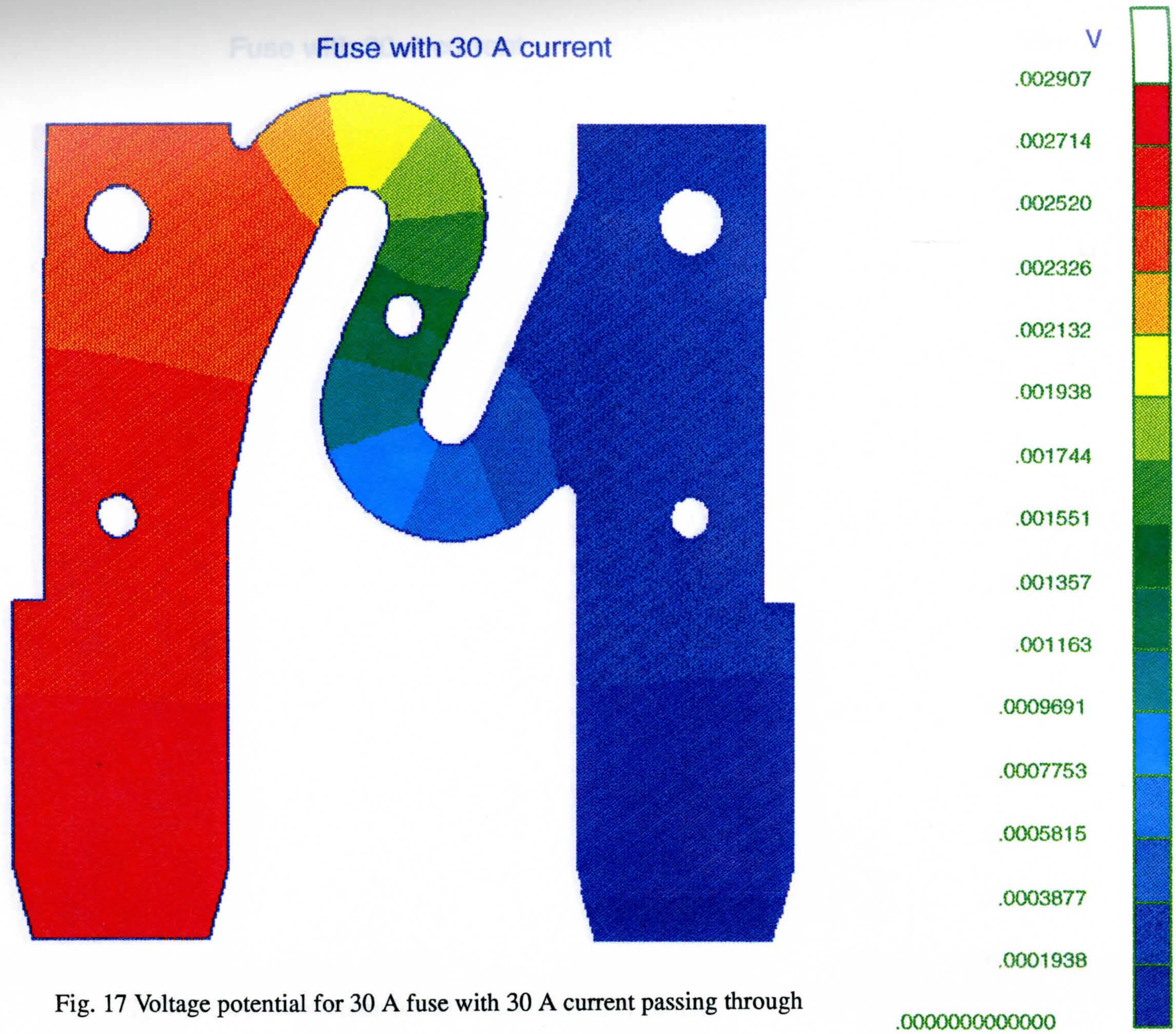

Fig. 17 Voltage potential for 30 A fuse with 30 A current passing through

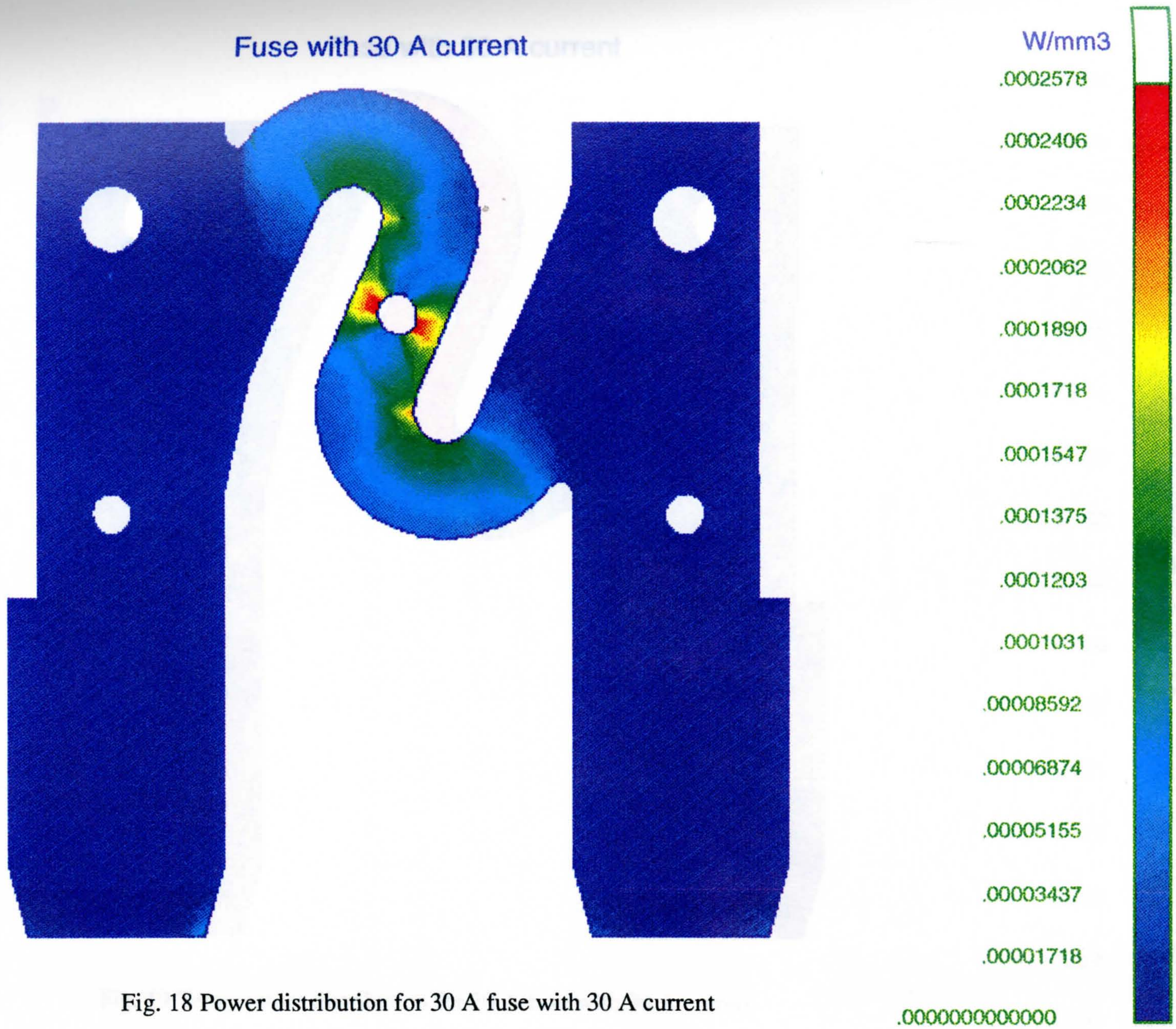

Fig. 18 Power distribution for 30 A fuse with 30 A current

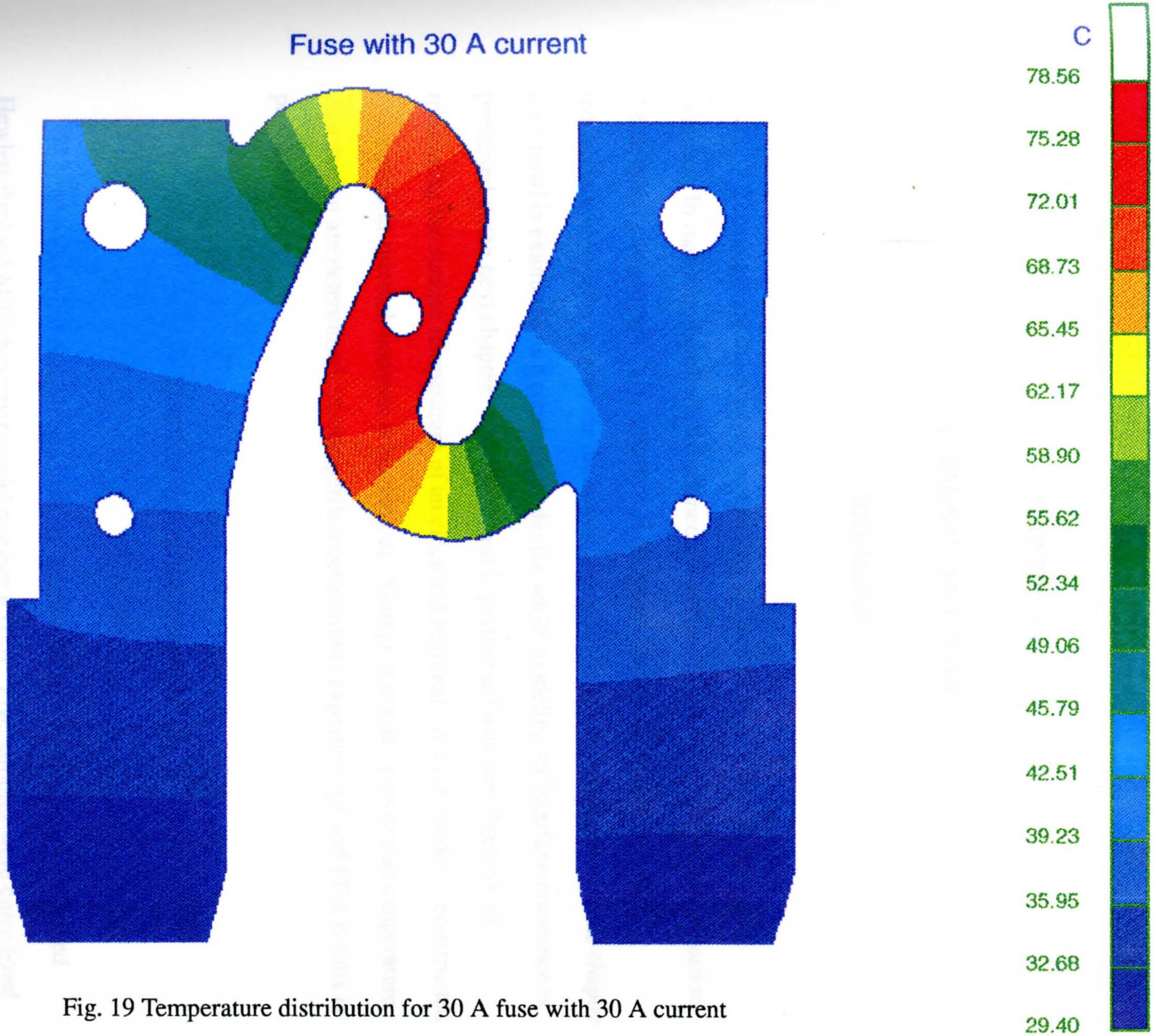

Fig. 19 Temperature distribution for 30 A fuse with 30 A current

CHAPTER IV

TERMINAL ANALYSES

Introduction

Terminals are the primary connectors to devices in automotive electrical systems. In many applications, the connection system is only as good as the connection the terminal can provide. The interface of a terminal is carefully designed and manufactured in order to provide the lowest electrical interface resistance. In this chapter a terminal is examined as a stand-alone device while modeling its interface resistance is presented in the next chapter. An experiment is performed with the objective of measuring the surface temperature of an electrical terminal. A FEA model is constructed and electrical-thermal analyses is carried out. Voltage potential, power and temperature distribution are determined. A comparison between the experimental and FEA results is provided.

Electrical Resistance Measurements

The electrical resistance across the terminal is measured using a calibrated Hewlett Packard Milliohmmeter model number 4328A. Five samples were considered and readings were taken at room temperature. The measurements and their average are shown in Table 10. The resistance is measured from the points of contacts between the fuse blade and the terminal and the average is found to be .44 mΩ. The locations of the points of measurements are shown in Table 10.

TABLE 10

TERMINAL RESISTANCE MEASUREMENTS

Sample #	R Value	Fuse Sample
1	0.00041 Ω	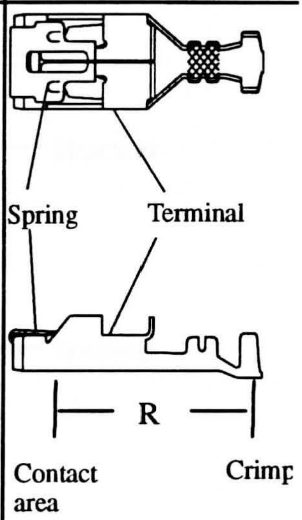
2	0.00043 Ω	
3	0.00045 Ω	
4	0.00044 Ω	
5	0.00047 Ω	
Average	0.00044 Ω	

Terminal Experiment

Description

The objective of the experiment is to obtain the surface temperature of the terminal in order to verify the FEA results. Surface temperature measurements of a horizontal terminal isolated from air movements around it were obtained. The terminal contact points were kept at a constant temperature while supplied by a steady current.

Temperature measurements of the location of the contact points were later applied to the FEA model as boundary conditions.

The terminal was tested at 10, 30 and 50 A currents. Temperature measurement locations are shown in Figure 7. To isolate the terminal from the surrounding air movements, it was placed in a small boaster board box. Since the Infrared camera cannot capture the image through the box, a window was cut in one side of the box for temperature readings. Plastic wrap was used to cover the window.

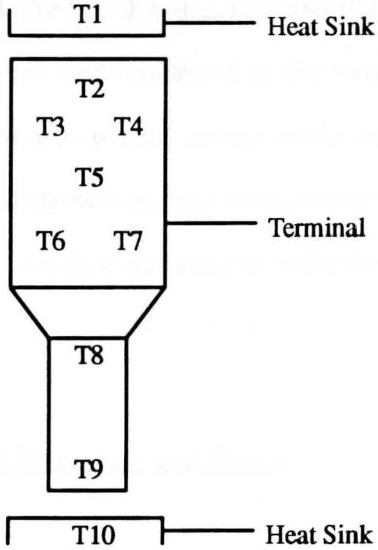

Fig. 20 Temperature measurement locations for the terminal experiment

The terminal was placed in a horizontal orientation. Two heat sinks were connected to the terminal in order to keep the contact point locations at a constant temperature. The current was kept steady by manually adjusting the power supply while measuring the current across a shunt resistor throughout the experiment. Ambient thermometer was placed in the lab near the experiment set up to measure the room temperature. The Inframatrics model 600 infrared imaging camera was used for the terminal temperature measurements.

Preparation

The experiment components were assembled on a wooden board. The board and the experiment set up is shown in Figure 21. First, the heat sinks were fixed to the board at such a distance that the terminal and the copper strips would fit horizontally between the heat sinks. The terminal contact points shown in Table 10 were soldered to the copper strips which in turn were soldered to the heat sinks so that the terminal would lie in a horizontal position. Two end wires were soldered on the two heat sinks for power supply purposes. The boaster board box was placed on top of the fuse. The test assembly was placed on a counter and the power supply was connected. The infrared camera was turned on and aimed at the window opening in order to gather the sample data required.

Experiment Procedure and Result

The power supply was turned on and adjusted for a 10 A steady current to pass through the terminal. After about 10 minutes, the temperature of the terminal stabilized and reached a steady state. The heat sink temperature was monitored to confirm constant temperature. The infrared camera was directed at the terminal and focused. The different data points on the fuse were measured and sample readings gathered. The temperature of the two heat sinks were also recorded. A set of three readings was taken for every data point. The average of the three readings was calculated and reported in Table 11.

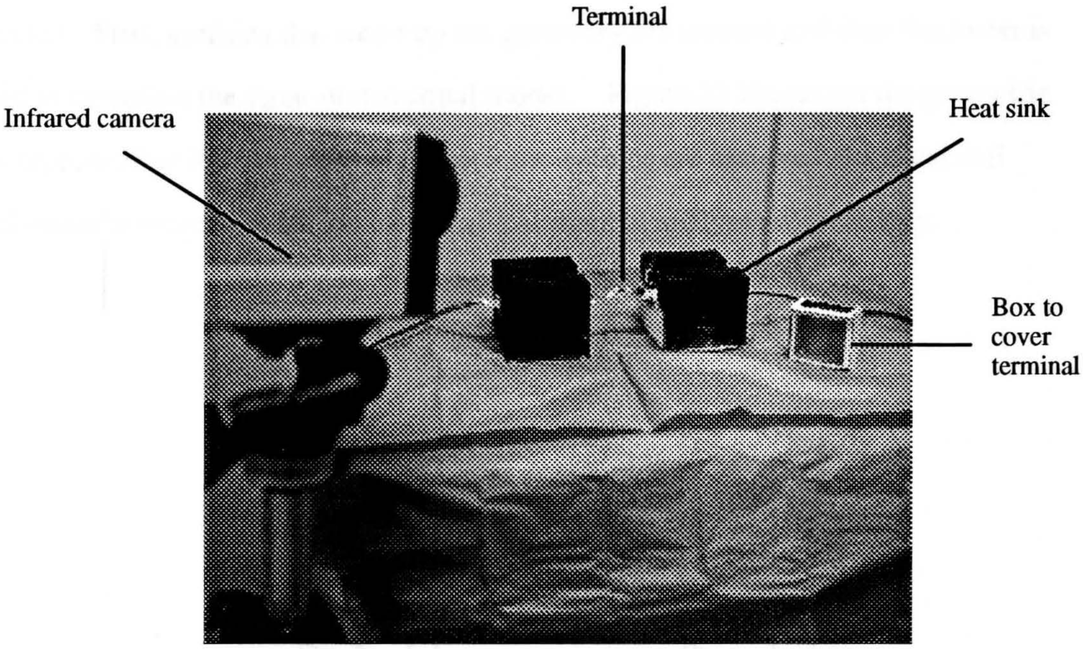

Fig. 21 The Terminal Experiment Set Up

The Finite Element Geometry Model

The actual terminal geometry has many fine details, shown in Figure 22. A finite element model that has all the details would be too large and would require a great deal of computer resources. As with any finite element modeling problem, simplifications should be made in order to minimize the modeling process as long as the model integrity is maintained. A simplified geometry is computed for the terminal model. First the terminal was weighted out and its volume calculated using its material density. The simplified model shown in Figure 22 preserves those of the terminal geometric characteristics that are important for heat transfer process. The length of the model is kept the same for conduction and its surface area is calculated and kept the same for both radiation and convection. The various surfaces of the terminal model were given thickness so that its volume is modeled accurately. A three-dimensional model is constructed. First, surfaces that make up the geometry are created and then thickness is assigned to complete the three-dimensional model. Figure 22 illustrates the geometric entities representing the terminal. The geometric entities are assigned electrical and thermal material properties for the electrical and thermal analyses respectively.

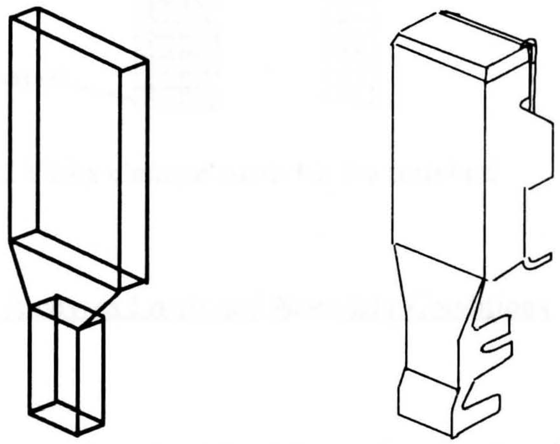

Fig. 22 Terminal geometry model

The Finite Element Mesh Model

The geometry is meshed as two-dimensional shell elements. Because the material properties and model thickness are assigned to the geometry underlying the elements, it is automatically associated with the mesh in Patran 3 software. This saves valuable analyses time when the need to further refine the mesh arises. The finite element mesh model is shown in Figure 23.

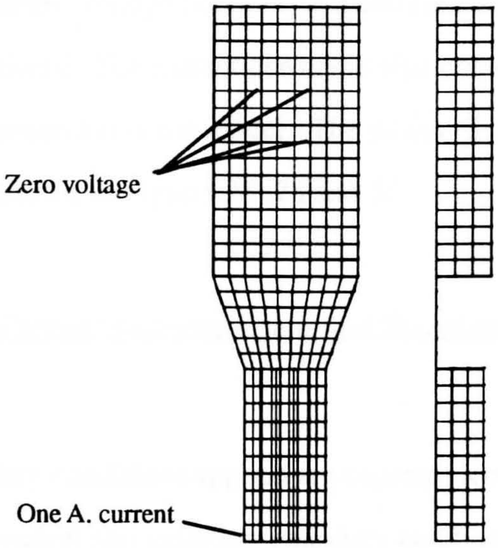

Fig. 23 Finite element mesh for the terminal

Electrical Analyses Loads and Boundary Conditions

The electrical-thermal analogy is utilized for performing the electrical analyses using the thermal analyses software. Only 1 A current is applied to the model so the voltage drop resulting from the analyses would equal the resistance value which is then compared with the terminal resistance measurement shown in Table 10. The boundary conditions applied to the model is a 1 A current and a grounded point represented as zero voltage. The current is applied on four nodes with a value of .25 as concentrated heat flux at the bottom of the terminal. The grounded points are specified as zero temperatures applied at the contact points as shown in Figure 23.

Electrical Analyses Results

The voltage potential difference is found to be 0.00042 v at room temperature. This translates to a 4.55% difference from the measurement obtained by the Hewlett

Packard Milliohmmeter. Voltage potential is illustrated on Figures 24, 27, and 30 for 10, 30 and 50 A respectively. The current density is also obtained and used to calculate the power distribution generated in the model. The power distribution for the different current densities is shown in Figures 25, 28 and 31.

Thermal Analyses Loads and Boundary Conditions

The boundary conditions applied are constant temperature, convection and radiation. The convection and radiation boundary conditions are applied to the outer faces of the terminal with the temperature dependant convective heat transfer coefficient[19] taken to be:

$$h_c = 0.61\left(\frac{\Delta T}{L^2}\right)^{1/5} \tag{14}$$

where h_c is the convective heat transfer coefficient, W/mm^2 and

L is the horizontal dimension, mm

The radiation boundary conditions are defined on the outer surface of the insulation by specifying the radiation heat transfer coefficient using the following equation[20]:

$$h_r = \frac{\sigma\varepsilon(T_s^4 - T_\infty^4)}{(T_s - T_\infty)} \tag{15}$$

where h_r is the convective heat transfer coefficient, W/mm^2°C and

σ is the Stephan-Bolzman constant,

---

[17]Holman, Heat Transfer, p. 253

[20]Incropera, Fundamentals, p.25

ε is the material emissivity,

T_s is the surface temperature, °K,

T_∞ is the ambient temperature, °K

A constant temperature is applied to both the terminal bottom crimp area and the contact points. This temperature is obtained from the experimental procedure results. Table 11 shows the value of the temperature applied as sink 1 and sink 2 for the crimp and contact area respectively. The thermal load applied to the model is that of the joule power generated due to the current passing through. The heat generation in watts per unit volume is applied to each element of the model.

Thermal Analyses Results

The temperature distribution of the fuse blades and element are depicted on Figures 26, 29 and 32 for 10, 30 and 50 A respectively. The FEA results are shown in Table 11 for the various current density values. Table 11 also shows a comparison between the experimental and FEA results for the same locations. The accuracy of the FEA is calculated and depicted in the same Table. The finite element model results are in good agreement with the experimental results.

Discussion

The comparison in Table 11 shows better correlation of T_6, T_7, T_8 and T_9 than the rest of the temperatures. The reason for the difference in temperatures could be attributed to the upper FEA boundary conditions locations. The boundary conditions are imposed at the area close to T_2, T_3, T_4, and T_5. These boundary conditions are applied with the temperature value of T_1 which is the heat sink temperature. The boundary condition locations are the same as the points of zero voltage shown on Figure 23. This can explain the low temperatures in the locations around the boundary conditions points. A better boundary conditions location could be the temperature of T_2 applied at its location shown on Figure 20.

TABLE 11

TERMINAL RESULTS COMPARISON

Current	Method	Temperature °C / Node number												
		T1	T2	T3	T4	T5	T6	T7	T8	T9	T10	Sink1	Sink2	Ambient
10 Amps	Test	22.6	23.6	23.5	23.5	23.3	23.7	23.7	23.6	23.7	23.3	22.6	23.3	23.1
	FEA	B.C.	22.7	22.69	22.69	22.68	22.84	22.84	23.56	23.47	B.C			
	% diff		3.81	3.40	3.45	2.66	3.63	3.63	0.17	0.97				
30 Amps	Test	23.9	26.3	26.3	26.3	26.6	26.8	27.0	27.1	27.1	24.1	23.9	24.1	22.5
	FEA	B.C	24.22	24.21	24.21	24.27	25.25	25.25	28.79	26.28	B.C			
	% diff		7.91	7.95	7.95	8.76	5.78	6.48	6.24	3.03				
50 Amps	Test	24.9	32.0	32.0	32.2	32.0	32.8	33.0	34.0	33.1	25.6	24.9	25.6	23.4
	FEA	B.C	25.69	25.69	25.69	25.87	28.52	28.52	38.22	31.4	B.C			
	% diff		19.72	19.72	20.22	19.16	13.05	13.58	12.41	5.14				

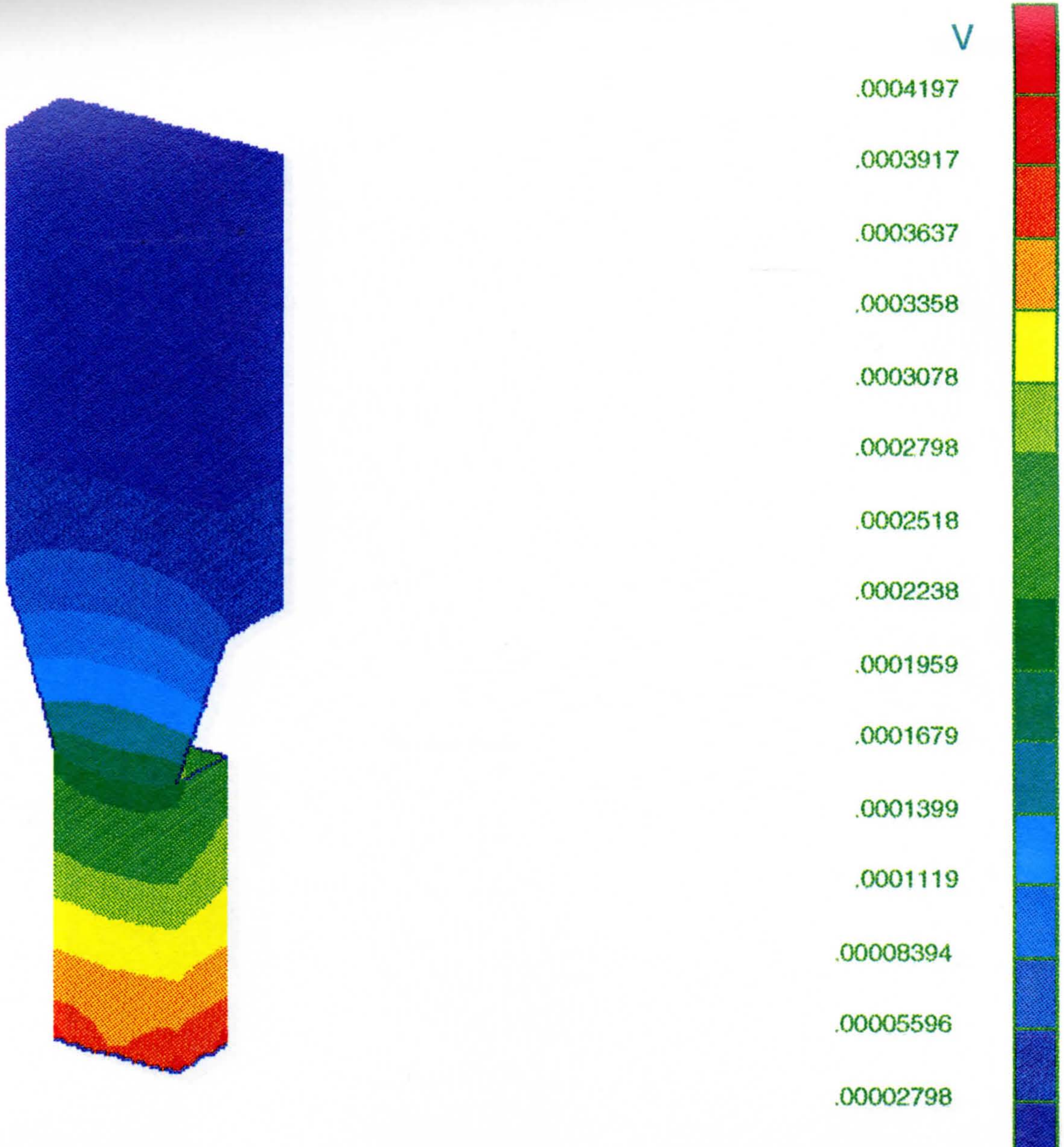

Fig. 24 Voltage potential for terminal with 10 A current

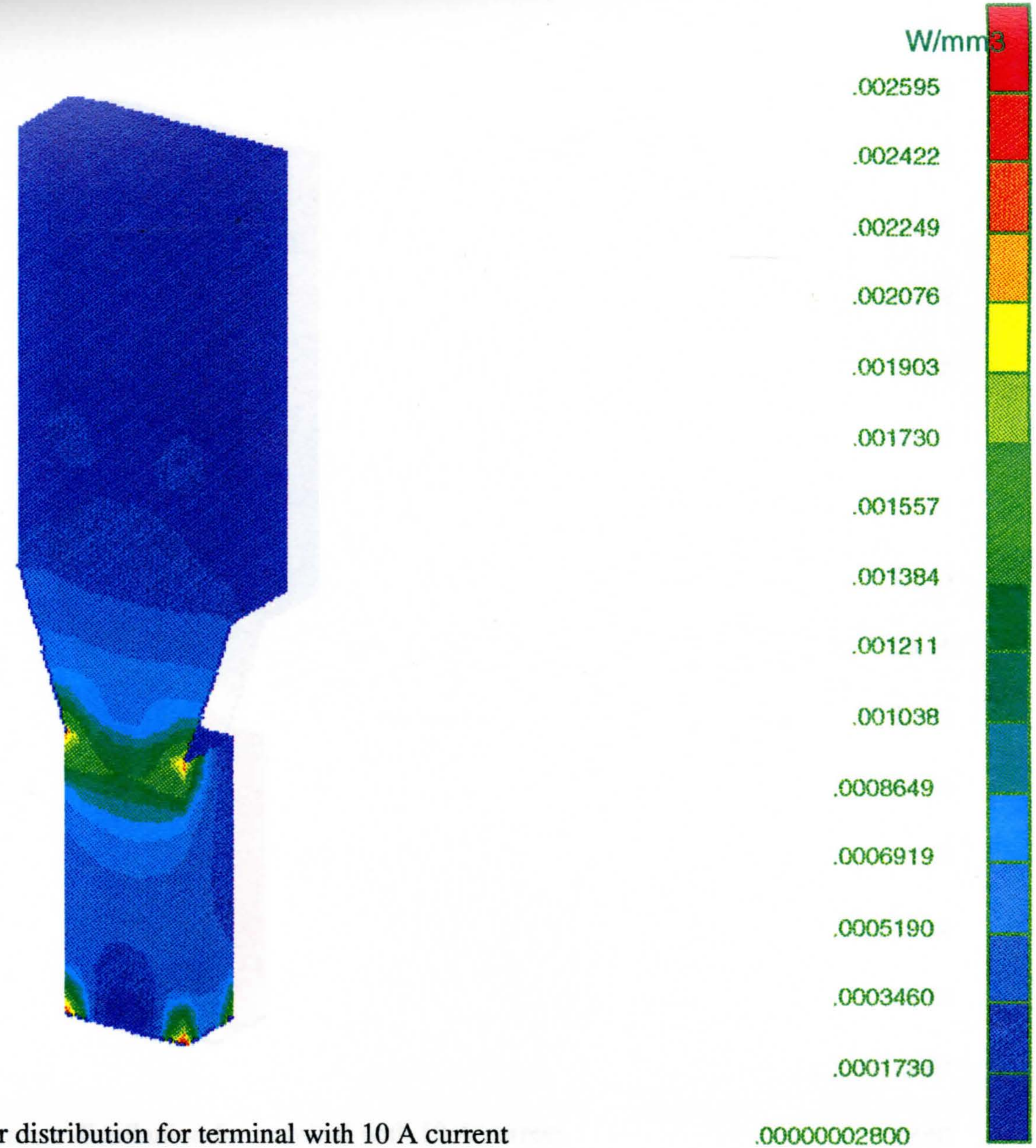

Fig. 25 Power distribution for terminal with 10 A current

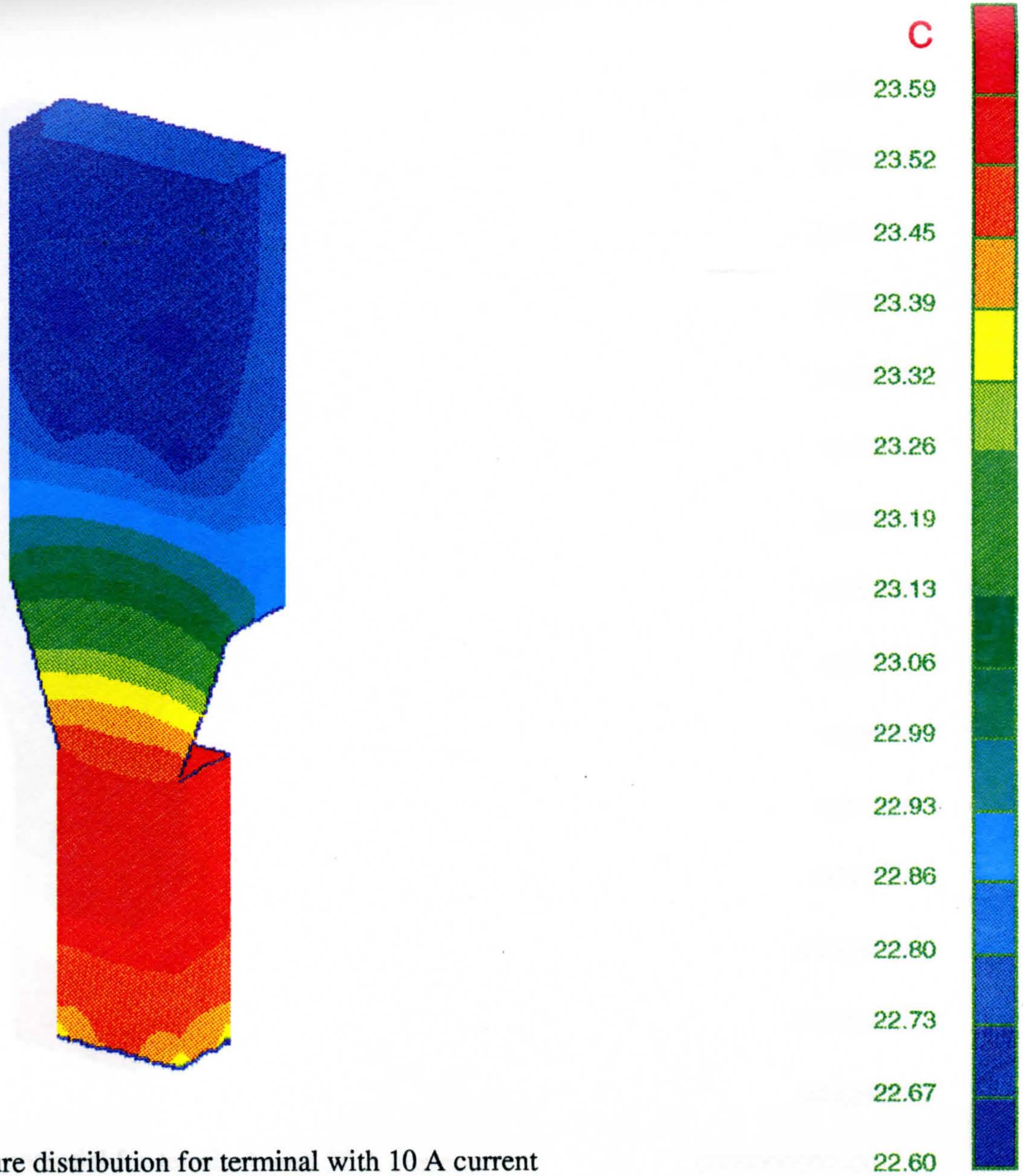

Fig. 26 Temperature distribution for terminal with 10 A current

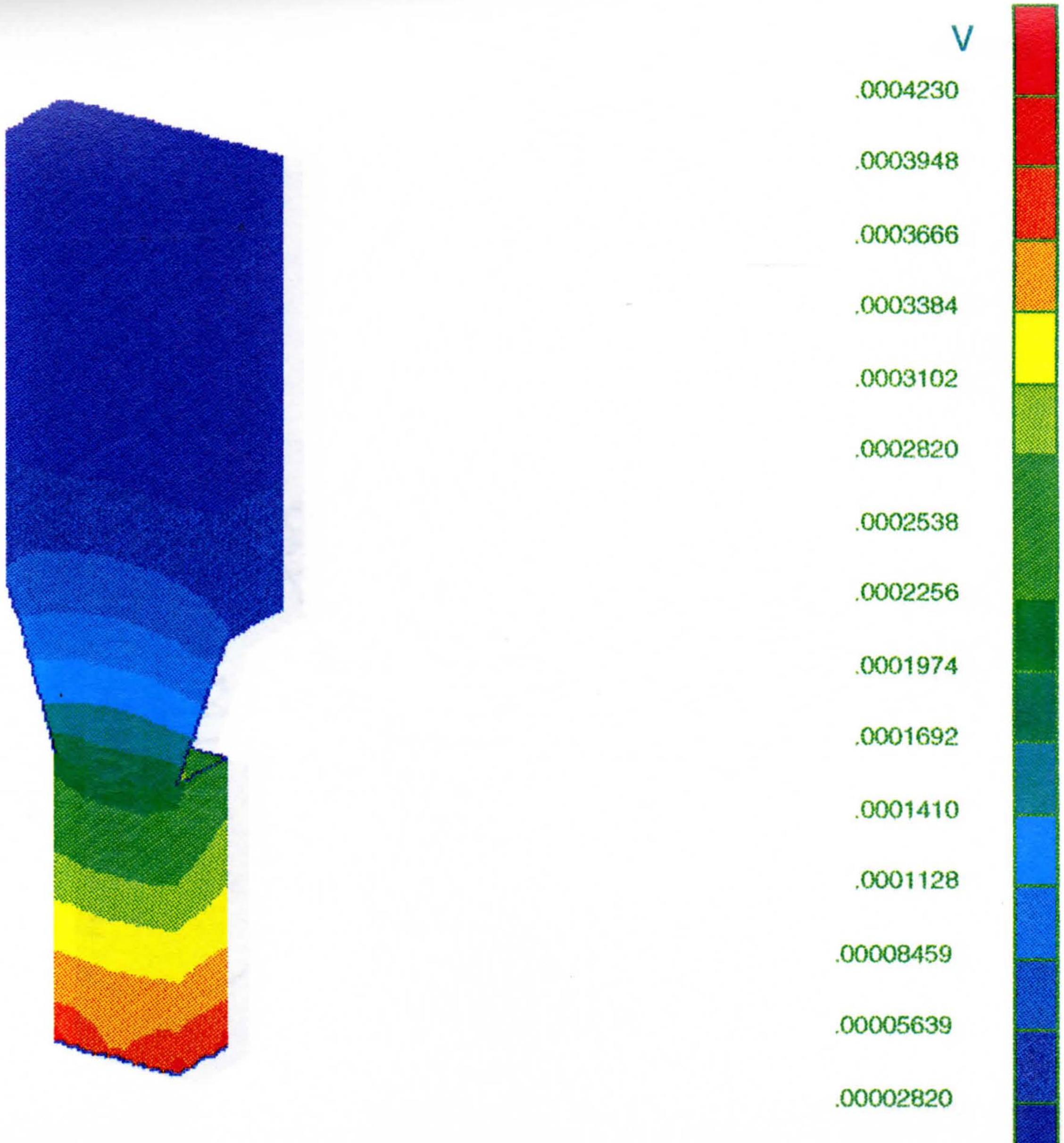

Fig. 27 Voltage potential for terminal with 30 A current

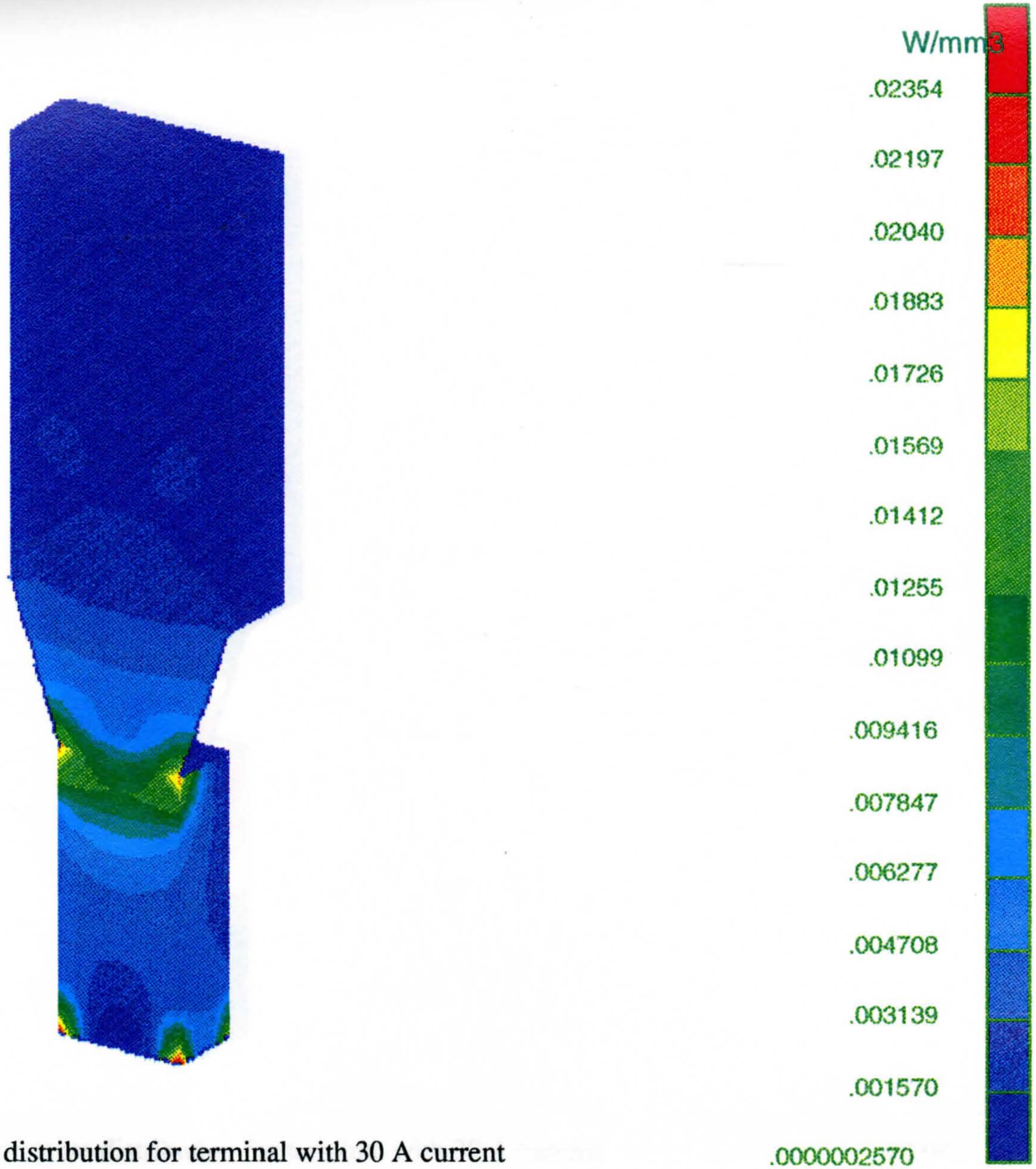

Fig. 28 Power distribution for terminal with 30 A current

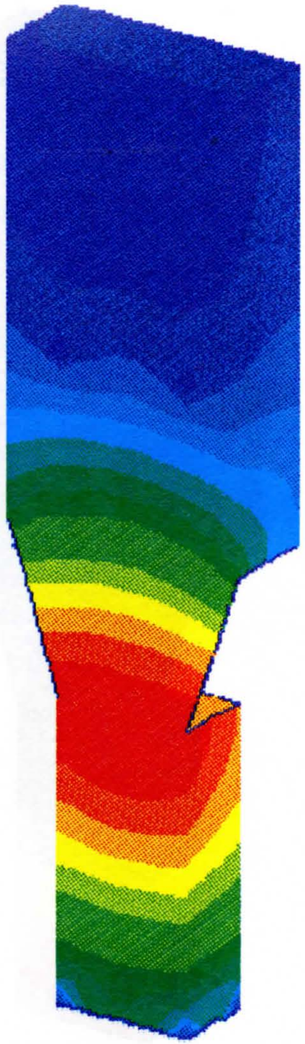

Fig. 29 Temperature distribution for terminal with 30 A current

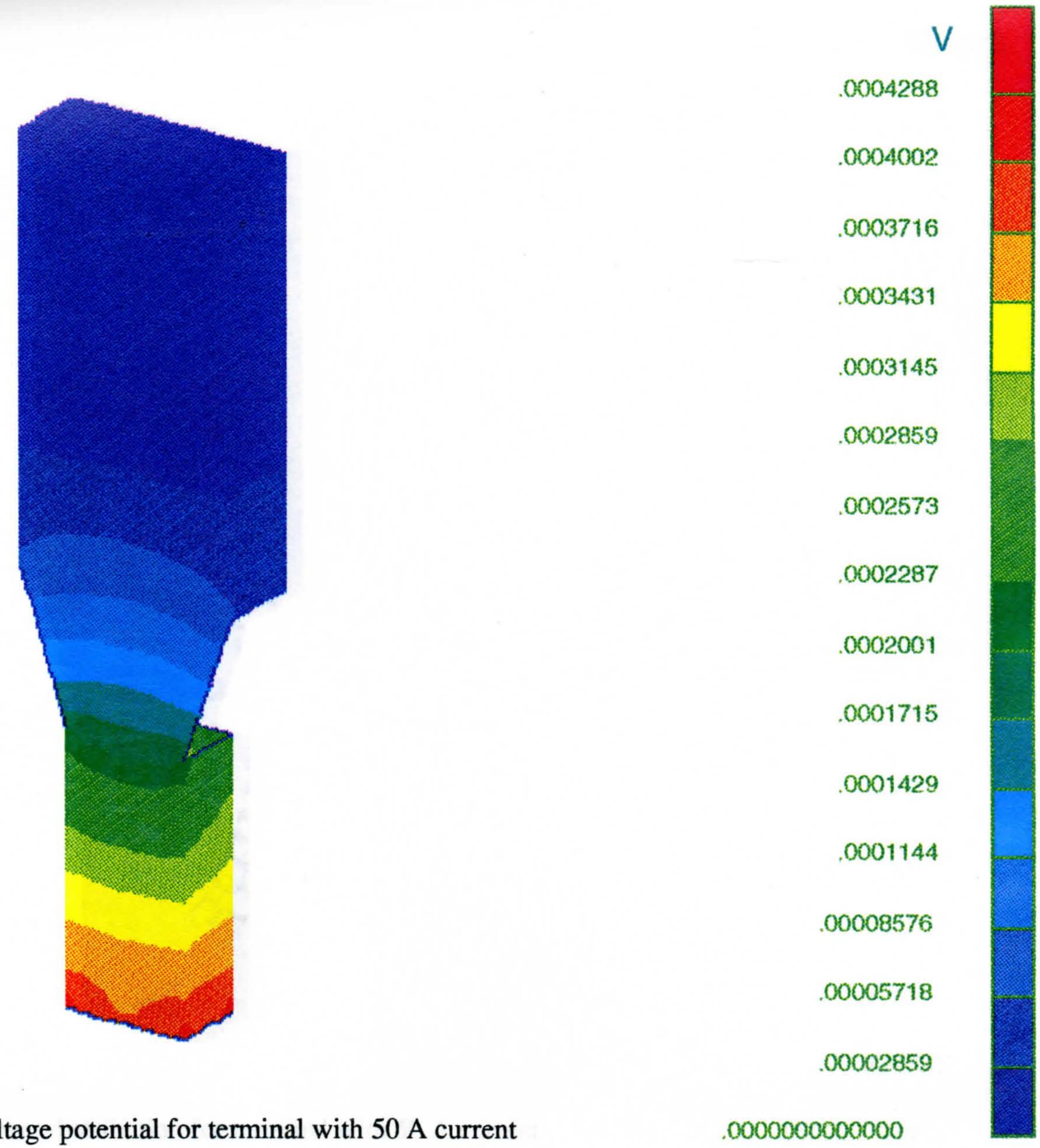

Fig. 30 Voltage potential for terminal with 50 A current

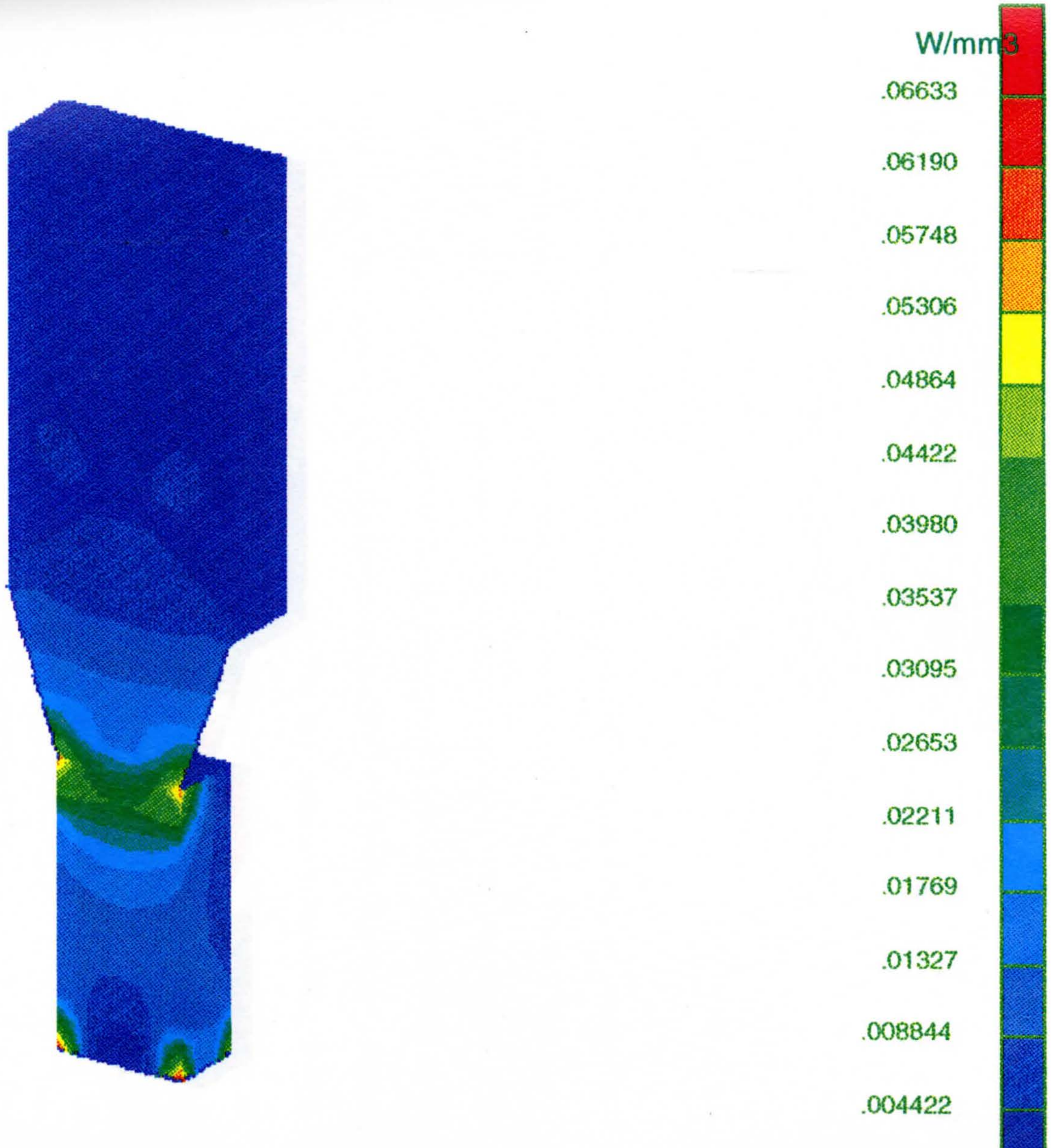

Fig. 31 Power distribution for terminal with 50 A current

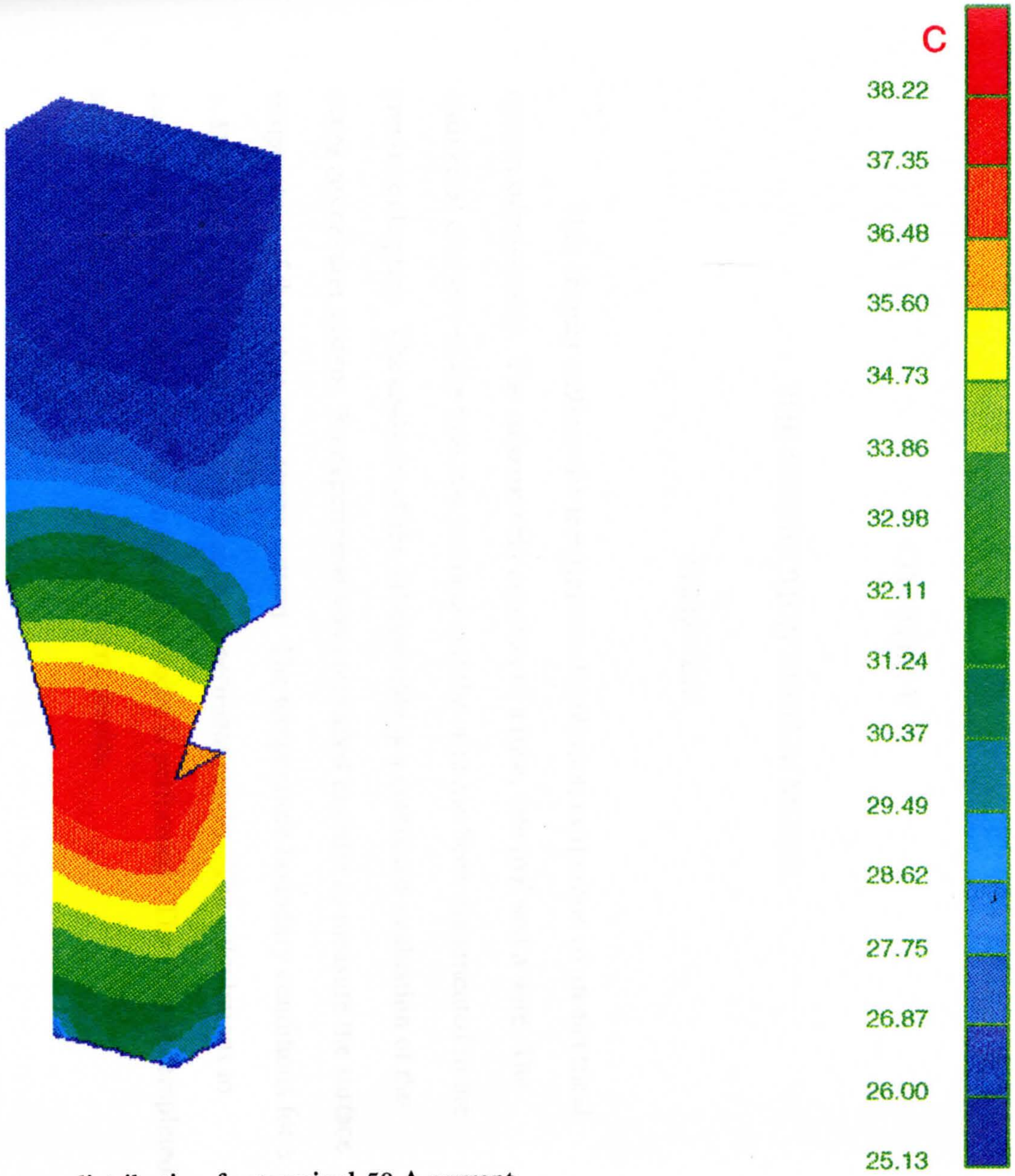

Fig. 32 Temperature distribution for terminal 50 A current

CHAPTER V

THE CONNECTION SYSTEM MODEL

Introduction

This chapter outlines the temperature distribution evaluation of an electrical system subassembly. The subassembly consists of a fuse, terminal and a wire. The individual analyses of the fuse, the terminal and the wire has been documented in the previous chapters. The analyses of the subassembly is a combined evaluation of the entire connection system. An experiment was conducted in order to measure the surface temperature of the entire connection system. The temperature boundary conditions for a 3–D finite element model is taken from the experiment results. The calculations to incorporate the contact resistance in the FEA model is performed. The FEA is completed and its results are compared with the experiment results.

After evaluating each component of the electrical system in a sub-analyses case, the entire connection system is now being evaluated. The results of this connection system analyses will provide the designer with the temperature distribution of the system placed in a given environment. The analyses takes into consideration the electrical and thermal interface resistance by incorporating a representative model between the terminal and fuse blades. Temperature dependent material properties are incorporated for the various components of the finite element model. First, the experiment is performed to gather the data for comparison and boundary conditions.

The Connection System Experiment

Description

The objective of the experiment is to obtain the surface temperatures of the connection system to verify the FEA results. The connection system is an electrical subassembly that consist of a fuse, two terminals and two wires. Current is passed through the assembly from one wire and out through the second wire. The two wire ends were kept at a constant temperature while the connection system is supplied by a steady current. The connection system components were kept isolated from air movements around it to only allow the natural convection effects to take place. Temperature measurements of the various points of the subassembly were measured for 30 A current value. Temperature measurements of the soldered ends of the wires were later applied to the FEA model as boundary conditions.

Experiment Preparation

To ensure integrity of experiment, new and unused parts are used to assemble the connection system. The terminals are crimped onto the wires using a hand crimping tool then soldered to maximize the contact interface at the junction. The two terminals were then connected to the blades of a 30 A automotive fuse. The wires were soldered on two heat sinks. Two other wires were soldered to the other end of the heat sink for power supply. The fuse plastic housing is cut open using a razor blade. The housing is then removed with the help of a screw driver. The housing is taped back onto the fuse terminal and blades until the time the experiment is performed to prevent any damage to the thin fuse element.

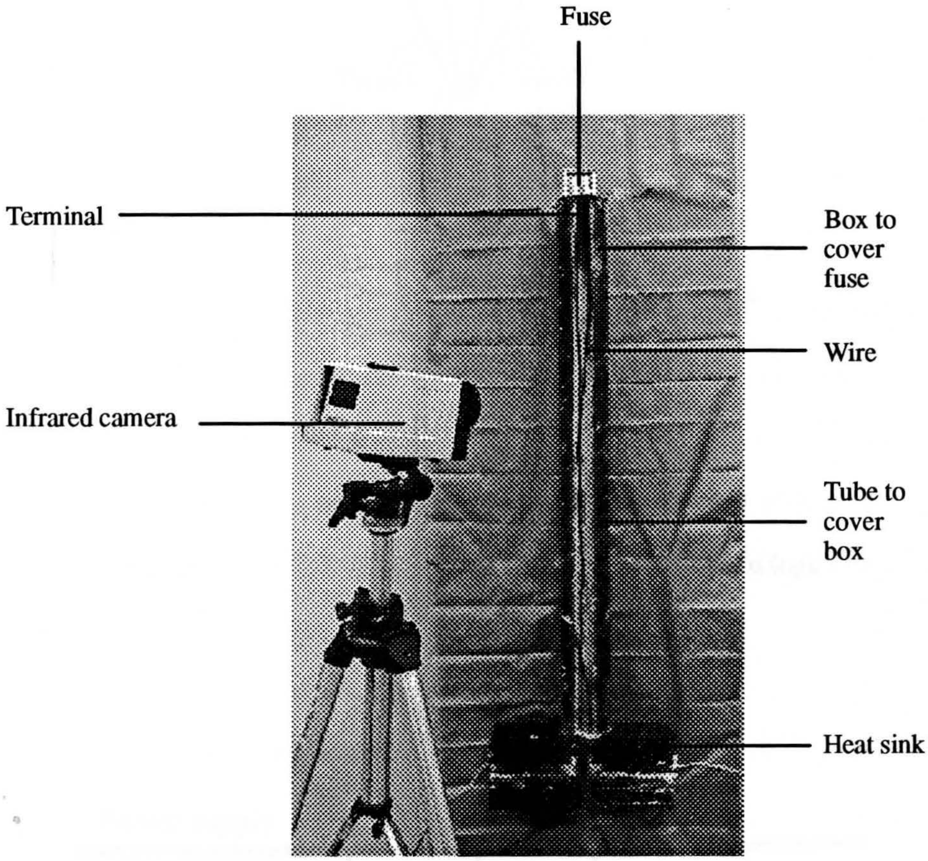

Fig. 33 Connection system experiment set up

The subassembly was tested at 10, 20 and 30 A currents. To isolate the fuse and the terminals from the surrounding air movements, it was placed in a small boaster board box. A window was cut in one side of the box for temperature readings. Plastic wrap was used to cover the window. To isolate the wire from the surrounding air movements, it was placed inside a tube. A window 13 mm wide was cut along the tube length and was covered with clear thin plastic wrap for visualization and temperature measurement. The tube was fixed on a wooden board for portability. The wire was placed in the center of the tube with it's ends outside.

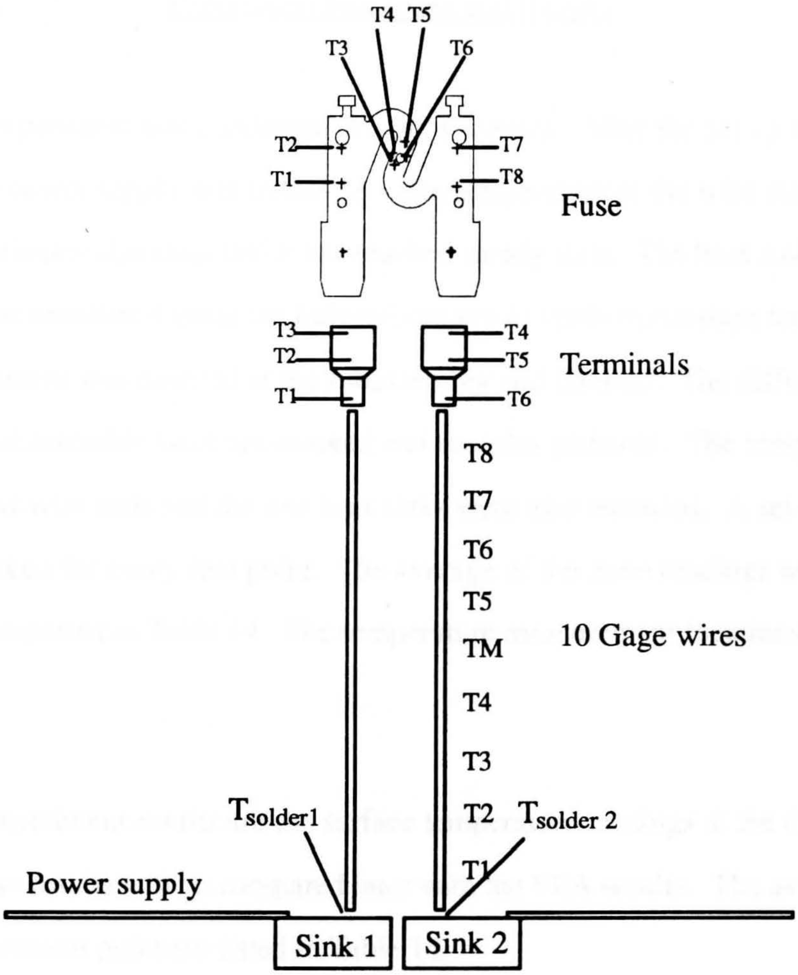

Fig. 34 Connection system temperature measurements locations

Two heat sinks were connected to the wires in order to keep their ends at a constant temperature. The current was kept steady by manually adjusting the power supply while measuring the current across a shunt resistor throughout the experiment. An ambient thermometer was placed in the lab to measure the room temperature. The Inframatrics model 600 infrared imaging camera was used to measure the surface temperatures of the assembly. A picture for the experiment set up is shown in Figure 33.

Experiment Procedure and Results

The experiment was conducted at a 30 A current. After the set up was completed, the power supply was turned on. The temperature of the wire stabilized after about twenty minutes signaling that it has reached steady state. The heat sink temperature was monitored using the infrared camera to confirm constant temperature. The infrared camera was directed at the subassembly and focused. The different data points on the subassembly were pre-marked and samples gathered. The temperature of the two soldered wire ends and the two heat sinks were also recorded. A set of three readings was taken for every data point. The average of the three readings was calculated and reported in Table 14. The temperature measurement locations are shown in Figure 34.

The experiment results are the surface temperature readings at the desired locations. These results will be compared later with the FEA results. The average values for each measurement point are listed in Table 14.

Contact Resistance Representative Model

When electric current passes through two members in contact with each other, a constriction resistance occurs. This resistance is due to the area where the current flows being constricted. Although the apparent contact area A may look relatively large, the contact actually occurs in a much smaller area, about 1% of the apparent area. This small area is called the contact area A_c and physically consists of many very small contact spots. The difference between the apparent area and the contact area is occupied by the fluid between the two surfaces and is called the void area A_V. It is imperative to determine the characteristics of such contact in order to build a finite element model that represents it. Specifically, the electrical resistivity, thermal conductivity as well as a representative volume should be determined.

Figure 35 shows two solid bars in contact with each other through a cylindrical contact spot. This shape will be used in the calculation of the contact spot model used in the FEA. Consider material *a*, in the Figure, to represent the fuse blade, while material *b* represents the terminal. If we know the electrical resistance R_e between the two surfaces, the radius of the cylinder cross section can be determined from equation[21] (16). The electrical resistance between the two surfaces was measured for 5 samples. The measurements and their average are given in Table 12.

TABLE 12

CONTACT RESISTANCE MEASUREMENTS

Sample #	R Value
1	0.00009 Ω
2	0.00007 Ω
3	0.00006 Ω
4	0.00007 Ω
5	0.00008 Ω
Average	0.000074 Ω

$$R_e = \frac{\rho}{2a} \tag{16}$$

[21]Ragnar Holm, Electric Contacts Theory and Application, (New York: Reprint, Springer-Verlag Berlin Heidelberg, Fourth Edition, 1981), p.16

where R_e is the contact spot electrical resistance, Ω

ρ is the contacting surfaces electrical resistivity, Ωmm,

a is the contact spot radius, mm

After determining the radius of a cylindrical contact spot, equation (17) can be used to calculate the equivalent electrical resistivity of the contact spot. The length of the contact spot can be determined from the material roughness factor. Assuming that both contact surfaces have the same coating made out of silver, this factor equals 0.000063mm for each surface.

$$R_e = \frac{\rho \times L}{\pi a^2} \tag{17}$$

Where R_e is the contact spot electrical resistance, Ω

ρ is the equivalent electrical resistivity of the contact spot, Ωmm,

L is the cylindrical spot length, mm and

a is the contact spot radius, mm

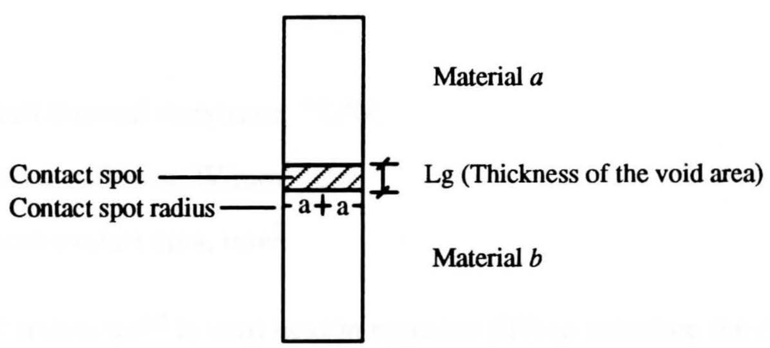

Fig. 35 Representation of a cylindrical contact spot

The only other quantity left to determine is the contact spot thermal conductivity. First the contact coefficient of heat transfer is calculated using equation (18)[22].

$$h_c = \frac{1}{L_g}\left(\frac{A_c}{A}\frac{2k_a k_b}{k_a + k_b} + \frac{A_v}{A}k_f\right) \tag{18}$$

where h_c is the contact coefficient, W/mm^2°C

L_g is the thickness of the void space, mm,

k_a is the thermal conductivity of material a, W/mm°C,

k_b is the thermal conductivity of material b, W/mm°C,

k_f is the thermal conductivity of fluid in void, W/mm°C,

A is the apparent contact area, mm^2,

A_c is the solid to solid contact area, mm^2,

A_V is the void area, mm^2,

This coefficient is used in equation (19)[23] in order to determine the thermal resistance R_{th}.

$$R_{th} = \frac{1}{h_c A} \tag{19}$$

where R_{th} is the contact thermal resistance, °C/W,

h_c is the contact coefficient, W/mm^2°C

A is the apparent contact area, mm^2

The thermal resistance[24] is used next in equation (20) to calculate the contact spot thermal conductivity. Figure 36 illustrates the representative cylindrical model and

---

[22]Holman, Heat Transfer, p. 47

[23]Holman, Heat Transfer, p. 48

[24]Holman, Heat Transfer, p. 48

it's equivalent cube for FEA purposes. The contact spot calculations are derived in appendix A and the results are provided in Table 13.

$$R_{th} = \frac{L_g}{k_c A_c} \tag{20}$$

where L_g is the thickness of the void space, mm,

R_{th} is the contact thermal resistance, °C/W,

k_c is the contact thermal conductivity, W/mm°C

A_c is the solid to solid contact area, mm^2

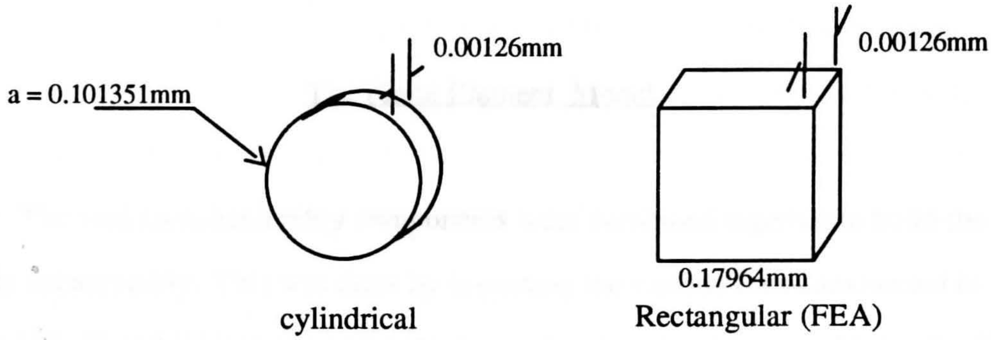

Fig. 36 Contact spot representation model

TABLE 13

CONTACT SPOT CALCULATION RESULTS

Characteristic	Value
radius, a	0.101351 mm
Contact area, A_c	0.032271 mm^2
Electrical resistivity, ρ	0.001895 Ω mm
Contact coefficient, h_c	0.725538 $W/mm^2{}^\circ C$
Thermal resistance, R_{th}	0.060009 °C/W
Thermal conductivity, k_c	0.651000 W/mm°C

The Finite Element Model

The various subassembly components were combined together to build the complete subassembly. This was done by importing the various files constructed in chapters VII, III and IV into one using the Patran 3 software. After combining the files together, some geometry functions might be needed in order to clear any interference between the different geometric entities. Connecting the various subassembly components together was done by using the ABAQUS multi-point constraint (MPC) feature. This feature allows for connecting any number of nodes to each other through connecting their degrees of freedom. In thermal analyses, this degree of freedom is the temperature. Once the subassembly component models are connected together, the model is ready to be assigned the new loads and boundary conditions.

Electrical Analyses

As was done in the previous chapters, the electrical-thermal analogy is utilized to perform the electrical analyses using the thermal analyses software. Electrical analyses is only performed on the conductive part of the model. A unit current is applied as a concentrated heat flux with a value of 0.25 on 4 nodes. The zero voltage potential is applied to the model as zero temperature. The loads and boundary conditions are combined together under one load case.

The analyses input file is prepared using the Patran 3 software. The entire FEA model is considered with the combined load case mentioned above. Several output options can be specified. The solution method chosen is a linear static, steady state solution. The results of interest are the heat flux at the element centroid and the nodal temperatures which represent the current density and the voltage potential respectively. The voltage potential is shown in Figure 37, while the Current distribution is shown in Figure 38.

Thermal Analyses

The final step in the procedure is the heat transfer analyses. Here the original finite element model used during the electrical analyses step is utilized. The loads, boundary conditions and material properties of the model are modified to reflect the thermal loads, boundary conditions and material properties. While in the electrical analyses step, only the electrically conductive part in the model is used; in the heat transfer step, the entire model including wire insulation is considered. The boundary conditions on the soldered ends of the wires is defined as a constant temperature. The constant temperature is obtained from experimental results and is given in Table 14 as the solder temperatures for the left and right wires. Convection and radiation boundary conditions are applied to the wire insulation surface. The temperature dependant convective heat transfer coefficient is defined according to the following equation[25]:

$$h_c = 1.42\left(\frac{\Delta T}{L}\right)^{1/4} \tag{21}$$

where h_c is the convective heat transfer coefficient, W/mm^2°C and

L is the vertical dimension, mm

The radiation boundary conditions are defined on the outer surface of the insulation by specifying the radiation heat transfer coefficient using the following equation[26]:

$$h_r = \frac{\sigma\varepsilon(T_s^4 - T_\infty^4)}{(T_s - T_\infty)} \tag{22}$$

where h_r is the convective heat transfer coefficient, W/mm^2°C and

σ is the Stephan-Bolzman constant,

ε is the material emissivity,

T_s is the surface temperature, °K,

T_∞ is the ambient temperature, °K

The power generation per unit volume calculated earlier is applied to each element of the model. Finally, the thermal conductivities of the different materials are assigned to the geometry model. The temperature dependency of the thermal conductivity is taken into consideration automatically by the abaqus software. After making all the necessary changes for the model, the ABAQUS heat transfer input file is

---

[25] Holman, Heat Transfer, p. 253

[26] Incropera, Fundamentals, p.25

generated using the Patran 3 software and then submitted to ABAQUS for analyses. The temperature distribution of the connection system is shown on Figure 39.

Discussion

A comparison between the experimental and FEA results is shown in Table 14. The table shows the temperatures for both the right and left hand side wires. It also shows the temperature distribution for the fuse and the terminal. The FEA results show general consistent agreement with the experimental results except for T_4, T_5 and T_6. In this area, the FEA temperatures have a significantly higher values than the experimental results. The difference can be attributed to several factors. The point of measurement of the infrared camera is not the same point exactly as the node in FEA. The measurement is taken only in the proximity of the node. A better convective heat transfer coefficient correlation than equation (21) could also improve the FEA results. Also, temperature loss through the plastic wrap film covering the connection system could account for some of the differences. However, the FEA results are within 10% accuracy. This difference is within the uncertainty normally associated with using heat transfer coefficient correlations.

TABLE 14

FUSE ASSEMBLY TEMPERATURE DISTRIBUTION CORRELATION

current, Amps.	Method	Temperature, °C													
		T1	T2	T3	T4	T5	T6	T7	T8	T9	T10	T12	Solder	Sink	ambient
Left Wire	Test	35.5		38.8	40.6		41.7	42.3		42.5	44.5	48.8	23.7	24.3	23.1
	FEA	34.3		38.25	39.54		40.02	40.22		40.39	40.76	44.78			
	diff. %	3.38		1.42	2.61		4.03	4.92		4.96	8.4	8.24			
Right Wire	Test	35.3		38.96	40.4		41.7	41.9		42.7	44.1	48.6	24.4	23.4	23.1
	FEA	34.87		38.96	40.36		40.88	41.11		41.3	41.69	45.76			
	diff. %	1.22		0.0	.1		1.97	1.89		3.28	5.46	5.84			
Fuse	Test	80.3	83.7		111	108	94.2	80	79						23.1
	FEA	82.45	86.97		128.3	126.9	129.2	81.57	81.02						
	diff. %	2.68	3.91		15.59	17.5	37.15	1.96	2.56						
Term	Test	59.6	71.4	69.4	70.6	70.2	60.1								23.1
	FEA	59.47	69.57	70.63	70.4	69.88	60.21								
	diff %	0.22	2.56	1.77	0.28	0.46	0.18								

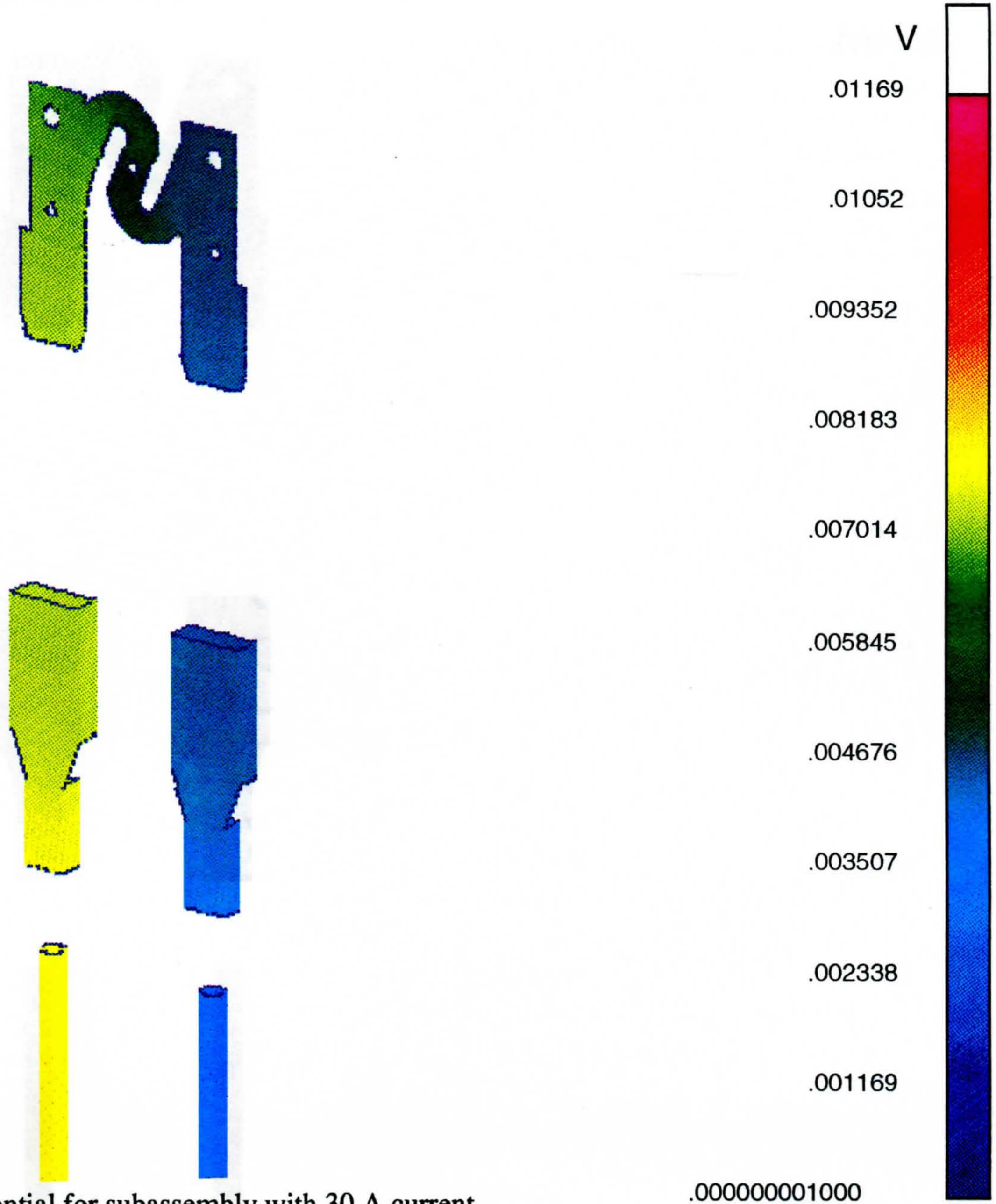

Fig. 37 Voltage potential for subassembly with 30 A current

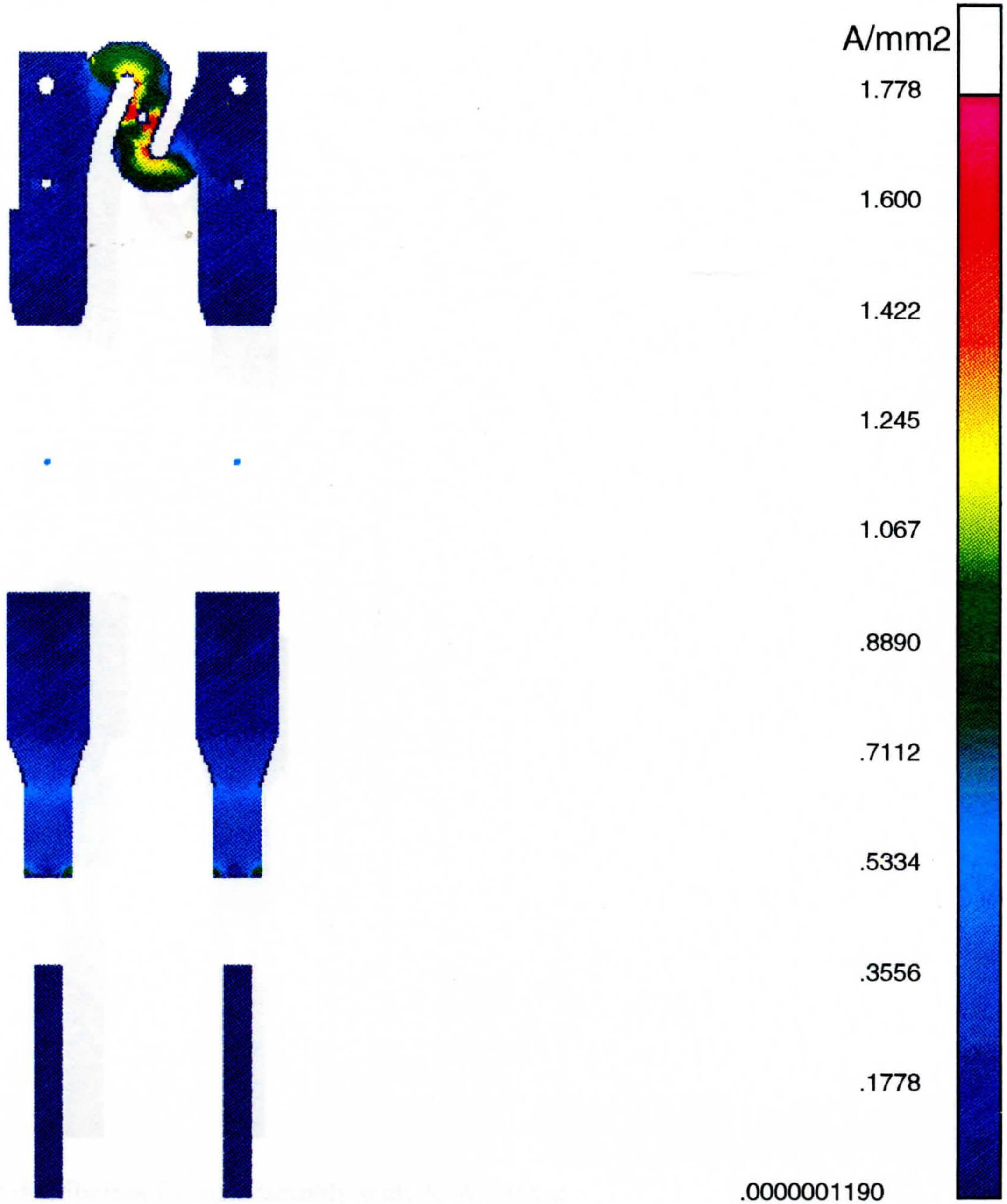

Fig. 38 Current distribution for subassembly with 30 A current

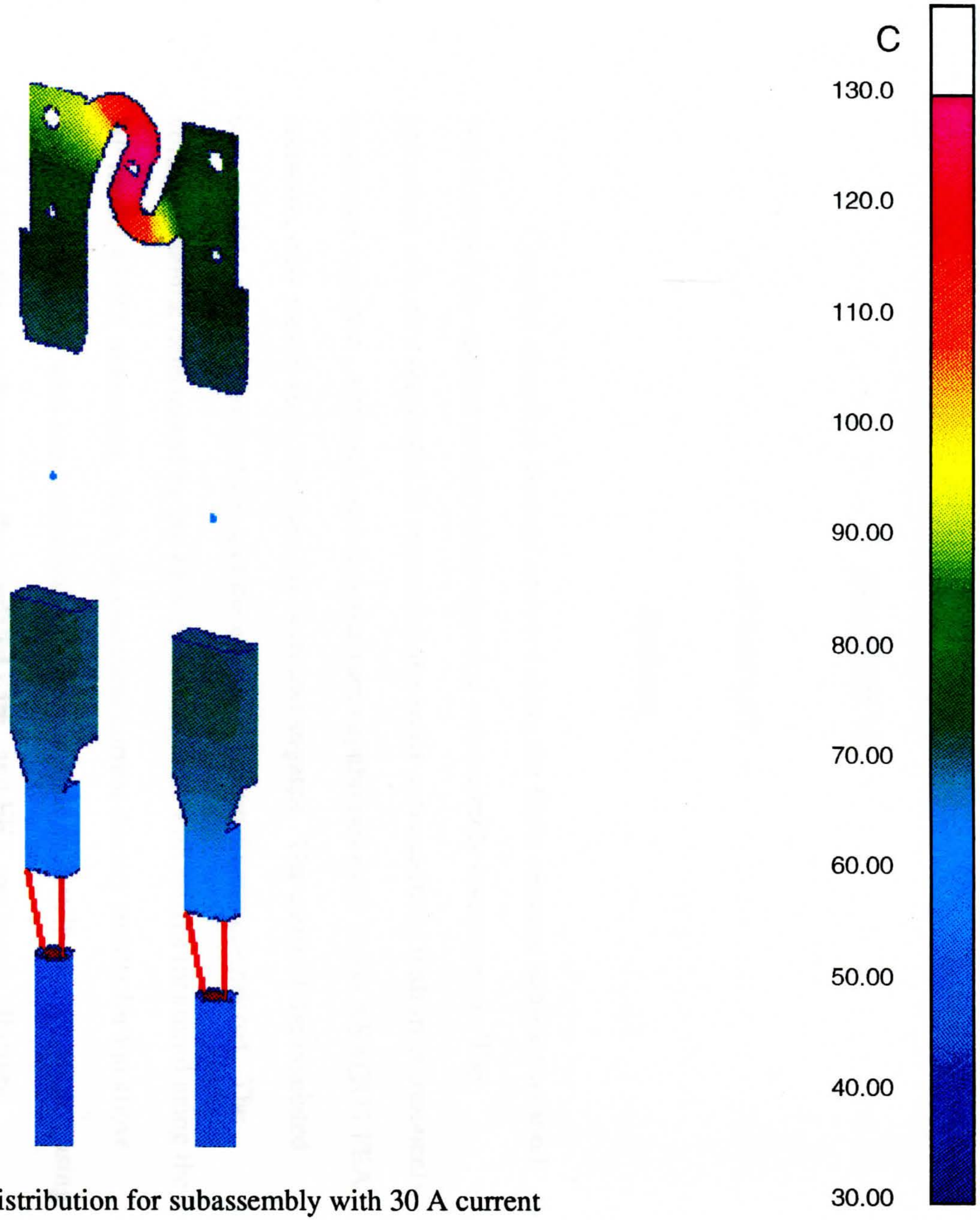

Fig. 39 Temperature distribution for subassembly with 30 A current

CHAPTER VI

SUMMARY

Findings

Coupled electrical-thermal analyses using the finite element analyses method was successfully applied to individual electrical subassembly components. The procedure was also successful in evaluating the entire sub-assembly with its components connected together. Although transient analyses capabilities exist in the ABAQUS FEA software, only steady state analyses has been investigated. The cases of the insulated wire model, the automotive fuse, and the electrical terminal were considered. The voltage potential determined by the FEA correlated well with results measured using the HP model 4328A ohmmeter. Also, the electrical current density results for the above components agreed with hand calculations. The temperature distribution computed using hand calculations, in the case of the insulated wire, and FEA method in all cases correlated well with test results using the Inframetrics model 600 infrared imaging camera. Results were found to be within 0 – 15% of the measured temperatures for electrical currents below 55 A.

Conclusions

It has always been a challenge to accurately measure the surface temperatures of objects with relatively small surface areas. One example is the automotive fuse where attachment of a thermocouple could affect its thermal characteristics. The use of the infrared imaging camera successfully determined the surface temperatures of the electrical subassembly and the components investigated. Also, the established Electrical–Thermal analyses approach using general purpose finite element analyses software produced results that correlated well with test and hand calculation results.

The difference between the experimental and the FEA results can be attributed to two areas. The first area is the updated electrical resistivity during an analyses iteration. At the beginning of the analyses the electrical resistivity is computed at an arbitrary temperature. The analyses method uses a convergence check between that temperature and the maximum calculated temperature for the model. The updated electrical resistivity for every subsequent iteration is based on the maximum temperatures found in the model for the various components. This electrical resistivity is applied to every element within the component regardless of the different temperatures of each element. The expected consequence of such application is to have more power generated at the lower temperature elements. Further research needs to be done to apply the temperature-dependent electrical resistivity for each element of the model. Finding a method within the ABAQUS software application to calculate the updated electrical resistivity for each element based on its resultant temperature from the previous thermal analyses step would help improve the accuracy of the results.

The second area is the calculation of the convection heat transfer coefficient. In this thesis work, an average temperature dependent heat transfer coefficient has been applied for the various areas of the model. The application of the local heat transfer coefficient has the potential of greatly improving the accuracy of the results. The prediction of the local heat transfer coefficients requires an additional analyses step using a computational fluid dynamics software. The resultant heat transfer coefficients would then be applied as boundary conditions for the thermal analyses ABAQUS model.

Recommendations

Finite element electrical analyses can be performed for complex geometry to determine current distribution and voltage drop using the ABAQUS software. In applications that require accurate prediction of power generated in its geometry due to electric current, this procedure proves successful. The coupled electrical-thermal analyses approach outlined in this thesis can be used to predict the surface temperature of electrical subassemblies. Innovative use of general purpose FEA software can help in solving many engineering problems. The coupled electrical-thermal analyses is a good example of such application.

APPENDIX A

MATHEMATICAL CALCULATIONS

Wire Calculations

Wire Electrical Analysis Calculations

From equation (41) :

$\rho = 2.28e^{-5}\ \Omega mm$,

l = 950 mm and

A = 5 mm^2

$$R = \frac{2.28 \times 10^{-5} \times 950}{5} = 0.043320\Omega \tag{23}$$

And from equation (40) :

$$P = (30)^2 \times 0.04332 = 38.9880W \tag{24}$$

Wire Thermal Analysis Calculations

Conduction:

From equation (44):

L = 910 mm

r_o = 1.9 mm

r_i = 1.26 mm and

$k = 1.8e^{-4}$W/mm°C

$$R_k = \frac{\ln\left(\frac{1.90}{1.26}\right)}{2 \times \pi \times 910 \times 1.80 \times 10^{-4}} = 0.0399°C/W \tag{25}$$

Convection:

From equation (45):

$r_o = 1.9$ mm and

Assuming $h = .2e^{-4}$ W/mm^2°C

$$R_c = \frac{1}{2 \times \pi \times 910 \times 1.90 \times .2 \times 10^{-4}} = 0.46°C/W \tag{26}$$

Radiation:

Assuming $T_o = 40\ °C$, from equation (46):

$$R_r = \frac{(313.16 - 296.16)}{5.669 \times 10^{-14} \times 2 \times \pi \times 910 \times 0.8 \times 1.9 \times ((313.16)^4 - (296.16)^4)} = 1.7932°C/W \tag{27}$$

From equation (43):

$$\Sigma R_{th} = 0.0399 + \frac{0.46 \times 1.7932}{0.46 + 1.7932} = 0.406°C/W \tag{28}$$

From equation (47):

$$38.988 = \frac{T_i - 23}{0.406}$$

$$\Rightarrow T_i = (0.406 \times 38.988) + 23.0 = 38.8°C \tag{29}$$

Substituting back into equation (47):

$$T_o = T_i - \frac{q \ln\left(\frac{r_o}{r_i}\right)}{2\pi L k} = 38.8 - \frac{38.988 \times \ln\left(\frac{1.90}{1.26}\right)}{2 \times \pi \times 910 \times 1.80 \times 10^{-4}} = 37.2°C \tag{30}$$

We now iterate starting equation (27) to find out the new T_o:

Assuming $T_o = 37.2\ °C$, from equation (46):

$$R_r = \frac{(310.36 - 296.16)}{5.669 \times 10^{-14} \times 2 \times \pi \times 910 \times 0.8 \times 1.9 \times ((310.36)^4 - (296.16)^4)} = 1.8184°C/W \tag{31}$$

From equation (43):

$$\Sigma R_{th} = 0.0399 + \frac{0.46 \times 1.8184}{0.46 + 1.8184} = 0.407°C/W \tag{32}$$

From equation (47):

$$38.988 = \frac{T_i - 23}{0.407}$$

$$\Rightarrow T_i = (0.407 \times 38.988) + 23.0 = 38.9°C \tag{33}$$

Substituting back into equation (47):

$$T_o = T_i - \frac{q \ln\left(\frac{r_o}{r_i}\right)}{2\pi Lk} = 38.9 - \frac{38.988 \times \ln\left(\frac{1.90}{1.26}\right)}{2 \times \pi \times 910 \times 1.80 \times 10^{-4}} = 37.3°C \tag{34}$$

This temperature is within 0.27% of the temperature at the beginning of the iteration. The solution has converged.

Contact Spot Calculations

radius

To calculate the contact spot radius the following values are used in equation (16):

$R_e = 0.000074\ \Omega$,

$\rho = 1.5e^{-5}\ \Omega mm$,

$$0.000074 = \frac{15e^{-5}}{2a} \tag{35}$$

$a = 0.101351$ mm

Electrical resistivity

Substituting the following values into equation (17) :

$R_e = 0.000074\ \Omega$,

$L = 0.00063$ mm and

$a = 0.101351$ mm

$$0.000074 = \frac{\rho \times .00126}{\pi \times 0.101351^2} \tag{36}$$

$\rho = 0.001895\ \Omega\text{mm},$

Contact Coefficient

Substituting the following values into equation (18) :

L_g =0.00126 mm,

k_a = 0.428 W/mm°C,

k_b = 0.428 W/mm°C,

k_f = 0.031326 W/mm°C,

A = 22.968 mm^2,

A_c =0.032271 mm^2,

A_V =22.935729 mm^2,

$$h_c = \frac{1}{0.00126}\left(\frac{0.032271}{22.968} \times \frac{2 \times 0.428 \times 0.428}{0.428 + 0.428} + \frac{22.935729}{22.968} \times 0.031326\right) \tag{37}$$

h_c = 0.725538 W/mm^2°C

Thermal Resistance

From equation (19):

$$R_{th} = \frac{1}{0.725538 \times 22.968} = 0.060009\,°\text{C/W}, \tag{38}$$

Thermal Conductivity

From equation (20):

L_g = 0.00126 mm,

R_{th} = 0.06009 °C/W,

A_c = 0.032271 mm^2

$$0.060009 = \frac{0.00126}{k_c \times 0.032271} \tag{39}$$

$k_c = 0.651$ W/mm°C

BIBLIOGRAPHY

Baumeister, Theodore, Avallone, Eugene A. and Baumeister III, Theodore. Mark's Standard Handbook for Mechanical Engineers New York: McGraw–Hill, Inc., 1978.

Holman, J.P. Heat Transfer New York: McGraw-Hill, 1976.

Incropera, Frank P. and DeWitt, David P. Fundamentals of Heat Transfer New York: Wiley, 1981.

Kraus, John D. Electromagnetics. New Yourk: McGraw-Hill, Inc. Fourth Eddition, 1992.

Ress, Robert A. Jr., Application of The Finite Element Technique to The Thermal Analysis of a Conductive Medium subjected to Electrical Loading. Unpublished Master thesis, Youngstown State University, 1982.

Fuses for Automotive applications. The Netherlands: Littelfuse Tracor B.V., Utrecht [1989].

Andrews, J.A., Mahalingam L.M., and Berg, H.M. "Thermal Characteristics of 16–pin and 40–pin Plastic DIP's," IEEE Trans. Components, Hybrids, and Manufacturing Technology, CHMT–4, Dec. 1981, pp.455–461.

Waller, D.L., Fox, L.R. and Hannemann, R.J. "Analysis of Surface Mount Thermal and Thermal Stress Performance," IEEE Trans. Components, Hybrids, and Manufacturing Technology, CHMT–6, Sept. 1983, pp.257–266.

Lee, C.C., Palisoc A.L. and. Baynham, J.M.W. "Thermal Analysis of Solid State Devices using Boundary Element Method," IEEE Trans. Electron Devices, 35, pp.1151–1153.

Lee, C.C. and Palisoc, A.L. "Thermal Analysis of Semiconductor Devices," Topics in Boundary Element Research, Ed. by C.A. Brebbia, Berlin, Germany: Springer–Berlag, Vol. 7, 1990, pp.12–33.